JPET Fast Forward. Published on July 2, 2022 as DOI: 10.1124/jpet.122.001195
This article has not been copyedited and formatted. The final version may differ from this version.

JPET-AR-2022-001195R1

Physiological Characterization of the Transporter-Mediated Uptake of the Reversible Male Contraceptive H2-Gamendazole Across the Blood-Testis Barrier

Raymond K. Hau, Joseph S. Tash, Gunda I. Georg, Stephen H. Wright, and Nathan J. Cherrington

College of Pharmacy, Department of Pharmacology & Toxicology, The University of Arizona, Tucson AZ, USA (R.K.H. and N.J.C.)

KU School of Medicine, Department of Molecular & Integrative Physiology, The University of Kansas Medical Center, Kansas City, KS, USA (J.S.T.)

College of Pharmacy, Department of Medicinal Chemistry and Institute for Therapeutics Discovery and Development, The University of Minnesota, Minneapolis, MN, USA (G.I.G.)

College of Medicine, Department of Physiology, The University of Arizona, Tucson, AZ, USA (S.H.W.)

JPET-AR-2022-001195R1

Running Title: Physiological Characterization of H2-Gamendazole Transport

Corresponding Author:

Nathan J. Cherrington

1703 E. Mabel St., Tucson, AZ, 85721

(520)-626-0219, cherring@pharmacy.arizona.edu

Text Pages: 50

Number of Tables: 2 (+1 supplemental table)

Number of Figures: 6 (+4 supplemental figures)

Number of Supplemental Files: 1

Number of References: 88

Number of Words in Abstract: 250

Number of Words in Introduction: 802

Number of Words in Discussion: 2121

Abbreviations: BCRP: Breast cancer resistance protein, BTB: Blood-testis barrier, CNT: Concentrative nucleoside transporter, ENT: Equilibrative nucleoside transporter, GMZ: Gamendazole, H2-GMZ: H2-gamendazole, [^{3}H]E3S: [^{3}H]Estrone 3-sulfate, hT-SerC: Immortalized human Sertoli cell, IS: Internal standard, LC: Leydig cell, LC-MS/MS: Liquid chromatography-tandem mass spectrometry, MATE: Multidrug and toxin extrusion protein, MRM: Multiple reaction monitoring, MRP: Multidrug resistance-associated protein, OAT: Organic anion transporter, OATP: Organic anion transporting polypeptide, OCT: Organic cation transporter, OCTN: Organic cation transporter, novel,

PBS: Phosphate-buffered saline PMC: Peritubular myoid cell, P-gp: P-glycoprotein, SC: Sertoli cell, WB: Waymouth's buffer

Abstract

The blood-testis barrier (BTB) is formed by a tight network of Sertoli cells (SCs) to limit the movement of reproductive toxicants from the blood into the male genital tract. Transporters expressed at the basal membranes of SCs also influence the disposition of drugs across the BTB. The reversible, non-hormonal contraceptive, H2-gamendazole (H2-GMZ), is an indazole carboxylic acid analog that accumulates over 10 times more in the testes compared to other organs. However, the mechanism(s) by which H2-GMZ circumvents the BTB are unknown. This study describes the physiological characteristics of the carrier-mediated process(es) that permit H2-GMZ and other analogs to penetrate SCs. Uptake studies were performed using an immortalized human SC line (hT-SerC) and liquid chromatography-tandem mass spectrometry (LC-MS/MS). Uptake of H2-GMZ and four analogs followed Michaelis-Menten transport kinetics (one analog exhibited poor penetration). H2-GMZ uptake was strongly inhibited by indomethacin, diclofenac, MK-571, and several analogs. Moreover, H2-GMZ uptake was stimulated by an acidic extracellular pH, reduced at basic pHs, and independent of extracellular Na^+, K^+, or Cl^- levels, which are intrinsic characteristics of OATP-mediated transport. Therefore, the characteristics of H2-GMZ transport suggest that one or more OATPs may be involved. However, endogenous transporter expression in wild-type CHO, MDCK, and HEK-293 cells limited the utility of heterologous transporter expression to identify a specific OATP transporter. Altogether, characterization of the transporters involved in the flux of H2-GMZ provides insight into

the selectivity of drug disposition across the human BTB to understand and overcome the pharmacokinetic and pharmacodynamic difficulties presented by this barrier.

Significance Statement

Despite major advancements in female contraceptives, male alternatives, including vasectomy, condom usage, and physical withdrawal, are antiquated and the widespread availability of non-hormonal, reversible chemical contraceptives is non-existent. Indazole carboxylic acid analogs such as H2-GMZ are promising new reversible, anti-spermatogenic drugs that are highly effective in rodents. This study characterizes the carrier-mediated processes that permit H2-GMZ and other drugs to enter Sertoli cells and the observations made here will guide the development of drugs that effectively circumvent the BTB.

Introduction

Adjacent Sertoli cells (SCs) lining the periphery of the seminiferous tubules in the testes establish a network of intercellular junctional complexes that comprise the physical component of the blood-testis barrier (BTB) (Dym and Fawcett, 1970). Additionally, membrane transporters along the basal membranes of SCs influence the disposition of substances and constitute the physiological component of the BTB. These include uptake and efflux transporters such as the organic anion/cation transporters (OATs/OCTs/OCTNs), organic anion transporting polypeptides (OATPs), P-glycoprotein (P-gp), breast cancer resistance protein (BCRP), and multidrug resistance-associated proteins (MRPs). Consequently, the seminiferous tubule lumen can serve as a pharmacological sanctuary site because many endogenous and exogenous substances cannot effectively penetrate the tight epithelium formed by SCs and accumulate to affect post-meiotic spermatogenesis (Mruk et al., 2011; Klein and Cherrington, 2014; Mruk and Cheng, 2015; Miller and Cherrington, 2018). Additionally, the failure of some compounds that are intended to treat testicular diseases or disorders is largely affiliated with their inability to effectively penetrate the BTB. Therefore, it is essential for compounds designed to target the testes to also be potent substrates of uptake transporters and to not readily interact with efflux transporters expressed by SCs.

Vasectomy, condom usage, physical withdrawal, and the use of certain drugs are several of the current options for male contraception (Chao et al., 2014; Chao and Page, 2016). Vasectomy has a failure rate of <1% but is not immediately effective and

reversal can be unreliable without further assistance (Bernie et al., 2012). If used correctly, condoms have a 2% perfect-use failure rate, but are only used correctly 18% of the time (Trussell, 2011). Contraceptives such as dimethandrolone undecanoate, testosterone enanthate, trestolone, and others inhibit spermatogenesis; however, these drugs also cause hormonal imbalance or are irreversible in some cases (Gava and Meriggiola, 2019). Consequently, there is a need for a safer and reversible, non-hormonal contraceptive (Long et al., 2021). Adjudin, H2-gamendazole (H2-GMZ), and other indazole carboxylic acid analogs are currently being investigated as potential candidates for reversible, non-hormonal contraception and are likely to circumvent the BTB through transport proteins (Coulston et al., 1975; De Martino et al., 1981; Heywood et al., 1981; Grima et al., 2001; Gatto et al., 2002; Cheng et al., 2005; Tash et al., 2008a; Tash et al., 2008b; Su et al., 2009; Wang et al., 2010; Gupta et al., 2011; Holets et al., 2011; Mok et al., 2011; Su et al., 2011; Shoop et al., 2014). Adjudin has been described as a transported substrate for rat OCTN2, OATP1A5, OATP6B1, and OATP6C1, although nothing is known about the human transporters involved (Su et al., 2011). A single oral dose of H2-GMZ or gamendazole (GMZ) has been reported to specifically accumulate within the testes of rodents, rabbits and non-human primates to elicit a potent, reversible contraceptive effect (Tash et al., 2008a; Tash et al., 2008b; Gupta et al., 2011; Holets et al., 2011; Shoop et al., 2014). Despite these positive observations, H2-GMZ and GMZ have not been tested in humans.

Due to the chemical structure and predicted pK_a (4.33) of H2-GMZ, it is strongly ionized at physiological pH and cellular membrane penetration would likely require a carrier-mediated process. Moreover, studies have shown direct interactions between

H2-GMZ or GMZ with intracellular proteins such as HSP90 or eEF1A1, alluding to cell membrane penetration by a carrier-mediated process given its chemical structure and pK_a. H2-GMZ and GMZ have been shown to negatively affect F-actin cytoskeleton organization in cells, which may contribute to its anti-spermatogenic effect (Tash et al., 2008b; Sundar et al., 2020). Although H2-GMZ has been shown to inhibit OATP1B1- and OATP1B3-mediated transport, identification of the primary transporter-mediated processes has been unsuccessful (Shoop et al., 2014). Therefore, a comprehensive understanding of the transporter-mediated processes involved in the uptake of H2-GMZ and other analogs across the BTB is necessary to inform the development of future drug candidates that require male genital tract access.

This study aimed to identify the transporter-mediated pathway(s) for H2-GMZ penetration across the BTB due to its testes-specific accumulation, high efficacy *in vivo*, and physicochemical properties. The present study is the first to extensively characterize the mediated process(es) involved in the transport of H2-GMZ across epithelial cell membranes. The physiological characteristics of H2-GMZ transport were evaluated in primary rat SCs and a human SC line (hT-SerC) using liquid chromatography-tandem mass spectrometry (LC-MS/MS). Comprehensive characterization of H2-GMZ transport was performed in hT-SerCs, with partial characterization of other indazole carboxylic acid analogs. The characteristics of H2-GMZ transport suggest that one or more OATPs may be involved, although it is possible that other unknown transporters may share some activity. However, identification of the specific OATP isoform involved through overexpression of individual transporters was not feasible using CHO, MDCK, or HEK-293 cells. Ultimately, the results presented in

this study implicate a unique transporter-mediated pathway for drugs such as H2-GMZ to circumvent the BTB.

Methods

Reagents

All reagents were purchased from ThermoFisher Scientific (ThermoFisher Scientific, Waltham, MA, USA) or Sigma-Aldrich (Sigma-Aldrich, St. Louis, MO, USA) at the highest possible purity unless otherwise noted. H2-gamendazole (H2-GMZ), gamendazole (GMZ), JWS-2-112, JWS-2-176, RC-MC-100, and RC-MC-241 were synthesized in the laboratory of Dr. Gunda Georg from Department of Medicinal Chemistry of the University of Minnesota (Georg et al., 2010; Georg et al., 2013; Georg et al., 2015). The purity of all synthesized compounds was >95% as determined by HPLC analysis. The molecular weight of the conjugate base for each synthesized compound was used for calculating concentrations. All test compounds were solubilized in water, DMSO, or a mixture of both solvents and further diluted to working concentrations in the appropriate transport buffer. [^{3}H]Estrone 3-sulfate ([^{3}H]E3S, 48.9 Ci/mmol) was purchased from PerkinElmer (PerkinElmer, Waltham, MA, USA, Catalog #NET203250UC).

Animals

Procedures involving live rats were approved by the University of Arizona Institutional Animal Care and Use Committee. Nine-week-old Sprague-Dawley rats were purchased from Charles River Laboratories (Wilmington, MA, USA) and housed 2 per

cage in 12 hr on and off light cycles. Rats were given water and standard chow ad libitum. SC isolation for *in vitro* studies were completed after rats underwent a one-week acclimatization period. Rats were euthanized by CO_2 asphyxiation and death was confirmed with a diaphragm puncture.

Immortalized Human Sertoli Cell Cultures

Immortalized human Sertoli cells (hT-SerCs) were grown and maintained as previously described (Hau et al., 2020). Briefly, hT-SerCs were grown in DMEM/F12 (Sigma-Aldrich, St. Louis, MO, USA, Catalog #D8900) supplemented with 10 µg/mL human insulin, 2.5 ng/mL EGF, 10% fetal bovine serum, 1% penicillin–streptomycin, and 1 µg/mL puromycin in a 35°C humidified 5% CO_2 incubator. Cells were washed with Dulbecco's phosphate-buffered saline (PBS) during routine maintenance. All tissue culture-treated plates and flasks were coated with 2 µg/cm^2 poly-L-lysine (Sciencell, Carlsbad, CA, USA, Catalog #0413) before use.

Isolation and Maintenance of Primary Rat Sertoli Cell Cultures

Primary rat SCs were isolated from naïve 10-week-old Sprague Dawley rats as previously described with minor modifications (Legendre et al., 2010). Briefly, rats were euthanized by CO_2 asphyxiation and both testes were surgically removed and placed in sterile Dulbecco's PBS. The testes were detunicated, minced, and resuspended in DMEM/F12 supplemented with 10% fetal bovine serum and 1% penicillin–streptomycin before centrifugation for 10 min at 100 x *g*. The supernatant was discarded, and the process was repeated three times to partially clean up large tissue debris. Media

JPET Fast Forward. Published on July 2, 2022 as DOI: 10.1124/jpet.122.001195
This article has not been copyedited and formatted. The final version may differ from this version.

containing 2 mg/mL collagenase, 1 µg/mL soybean trypsin inhibitor, 10 µg/mL DNase, and 1 mg/mL hyaluronidase was added to dissociate and digest the tissue extracellular matrix for 30 min in a rocking water bath at 32°C. The digested tissues were centrifuged for 10 min at 100 x *g*, washed three times with media, passed through a 70 µM nylon mesh filter, and then through a 40 µM nylon mesh filter. The cells were plated on a 2 µg/cm^2 poly-L-lysine–coated cell culture flask and grown in DMEM/F12 supplemented 10 µg/mL human insulin, 2.5 ng/mL EGF, 10% fetal bovine serum, and 1% penicillin–streptomycin in a 35°C humidified 5% CO_2 incubator. Isolated cells underwent a hypotonic treatment (20 mM Tris-Cl, pH 7.4) to eliminate contaminating germ cells 24 hrs after isolation. Upon growing to confluency, primary rat SCs were passaged (up to and including passage 3) and used for downstream transport experiments.

Human Transporter Cloning

The open reading frame of human OATP2B1 was amplified from a pcDNA5/FRT-OATP2B1 vector using specific sense (5'-TTTAATGCTAGCATGGGACCCAGGATAGGGCCAGCGGGTGAGGTACCCCAGGTA-3') and antisense primers (5'-GTACGCGGCCGCTTACGTAGAATCGAGACCGAGGAGAGGGTTAGGGATAGGCTTACCCACTCGGGAATCCTCTGGCTT-3'). A NheI restriction enzyme site was added before the start of the ATG codon in the sense primer. A V5 epitope tag containing a 42 base pair sequence, TAA stop codon, and NotI restriction enzyme site were included after the end of the open reading frame in the antisense primer. The OATP2B1 gene insert was amplified by PCR with the appropriate primers using Apex 2X Taq Master

Mix (Genesee Scientific, San Diego, CA, USA, Catalog #42-133). PCR reactions were carried out with the following 3-step cycling conditions: initial denaturation at 95°C for 3 min followed by 35 cycles of denaturation at 95°C for 25 sec, annealing at 5°C below the T_m for 30 sec, and extension for 2 min at 72°C with a final extension for 10 min at 72°C.

The PCR products were gel purified and cut with the appropriate restriction enzymes. The constructs were subcloned into a NheI and NotI restriction enzyme-linearized pcDNA5/FRT Mammalian Expression Vector (Invitrogen, Carlsbad, CA, USA, Catalog #V601020) in a 3:1 insert to vector ratio with T4 DNA ligase (Invitrogen, Carlsbad, CA, Catalog #15224017). TOP10 competent *E. coli* cells were transformed with 2 µL of the reaction mixture by the heat shock method. Following bacterial transformation, culture, and purification, the plasmid was subjected to both restriction enzyme digestion with gel electrophoresis and Sanger sequencing with CMV forward and BGH reverse primers to confirm successful ligation.

CHO, MDCK, and HEK-293 Cell Cultures

CHO, MDCK, and HEK-293 cells were maintained as previously described (Zhang et al., 2004; Hotchkiss et al., 2015). Untransfected Flp-In CHO cells were grown in F12K (Sigma-Aldrich, St. Louis, MO, USA, Catalog #N3520) supplemented with 10% fetal bovine serum, 1% penicillin–streptomycin, and 100 µg/mL Zeocin in a 37°C humidified 5% CO_2 incubator. Untransfected Flp-In MDCK and HEK-293 cells were grown in DMEM (Sigma-Aldrich, St. Louis, MO, USA, Catalog #D5648) containing 10% fetal bovine serum, 1% penicillin–streptomycin, and 100 µg/mL Zeocin in a 37°C

humidified 5% CO_2 incubator. CHO cell lines stably expressing a human transporter were grown in the identical medium described above, except with 100 µg/mL hygromycin B instead of Zeocin. HEK-293-EV and HEK-293-OATP1A2 cells were obtained from Dr. Bruno Hagenbuch of the Department of Pharmacology, Toxicology & Therapeutics at the University of Kansas Medical Center (Kansas City, Kansas, USA). Both HEK-293-EV and HEK-293-OATP1A2 cells were grown in DMEM (Sigma-Aldrich, St. Louis, MO, USA, Catalog #D5648) containing 10% fetal bovine serum, 1% penicillin–streptomycin, and 2 µg/mL puromycin in a 37°C humidified 5% CO_2 incubator. HEK-293-EV and HEK-293-OATP1A2 cells were seeded on 50 µg/mL poly-D-lysine-coated (ThermoFisher Scientific, Waltham, MA, Catalog #A3890401) plates for all transport experiments. All cells were washed with standard PBS during routine maintenance.

Transfection of Human Transporters in CHO Cells

Stably overexpressing CHO-OATP2B1 cells were generated using the successfully ligated pcDNA5/FRT vector and Flp-In expression system (Invitrogen, Carlsbad, CA, USA, Catalog #K601002). Briefly, the ligated vectors were transfected into 70-80% confluent Flp-In CHO cells in 6-well plates using TurboFect Transfection Reagent (ThermoFisher Scientific, Waltham, MA, USA, Catalog # R0531). Twenty-four hours later, selection of antibiotic resistant and stable clones was performed using 500-600 µg/mL hygromycin B-supplemented media. Following initial antibiotic selection, the hygromycin B concentration was dropped to 100 µg/mL for routine culture.

Immunocytofluorescence Staining

HEK-293-EV, HEK-293-OATP1A2, Flp-In CHO, and CHO-OATP2B1 cells were grown on round glass coverslips to 80-90% confluence before fixation with 100% ice-cold methanol for 20 min. Non-specific epitopes in each sample were blocked using a solution of 5% goat serum in PBS containing 0.1% Tween 20 (PBS-T) for 30 min. Following epitope blocking, the coverslips were washed with PBS-T three times and the samples were probed with a V5 Tag Monoclonal Antibody (1:1000, Invitrogen, Waltham, MA, USA, Catalog #R960) or a DYKDDDDK (Flag) Tag Antibody (1:200, Cell Signaling Technology, Danvers, MA, USA, Catalog #2368S) diluted in PBS-T with 2% goat serum for 1 hr at room temperature. The coverslips were washed three times with PBS-T before probing with Alexa Fluor 488 Goat anti-Mouse IgG (H+L) Cross-Adsorbed Secondary Antibody (1:1000, Invitrogen, Carlsbad, CA, USA, Catalog #A-11001) or Alexa Fluor 488 Goat anti-Rabbit IgG (H+L) Cross-Adsorbed Secondary Antibody (1:1000, Invitrogen, Carlsbad, CA, USA, Catalog #A-11008) in PBS-T with 2% goat serum for 1 hr at room temperature. Coverslips were washed three times with PBS-T, then rinsed with water before counterstaining the nuclei using 1.5 µg/mL DAPI for 5 min. Following nuclei staining, the coverslips were washed three times with PBS and rinsed once with water before mounting onto glass slides using ProLong™ Diamond Antifade Mountant (Invitrogen, Carlsbad, CA, Catalog #P36970).

Slides were imaged using a Leica SP5-II confocal microscope (Leica Camera AG, Wetzlar, Germany) with a HC PL APO 40x/1.25 GLYC CORR CS2 objective (Leica Camera AG, Wetzlar, Germany). The image representing the green channel for Alexa Fluor 488-stained proteins and the image representing the blue channel for DAPI-

stained nuclei were superimposed to generate the final merged image for each figure. The HEK-293-EV and Flp-In CHO cells did not exhibit a fluorescent signal when probed with the V5 or Flag antibodies. Images were cropped from the original image to illustrate clearer staining patterns.

Transport Assay by LC-MS/MS

Total drug accumulation in cells was quantified using liquid chromatography coupled with tandem mass spectrometry. Briefly, cell cultures were grown in 24-well plates to confluence before transport experiments were performed for each compound. Test compounds were diluted into Waymouth's buffer (WB; 135 mM NaCl, 28 mM D-glucose, 13 mM HEPES, 5 mM KCl, 2.5 mM $CaCl_2$•$2H_2O$, 1.2 mM $MgCl_2$, 0.8 mM $MgSO_4$•$7H_2O$, pH 7.4) and the resulting mixture was added to each well for the indicated amount of time unless otherwise noted. WB was also prepared at pH 6.0, 6.5, 7.0, 7.5, and 8.0 to determine H^+-dependency in total uptake. Choline buffer (135 mM choline chloride, 28 mM D-glucose, 13 mM HEPES, 5 mM KCl, 2.5 mM $CaCl_2$•$2H_2O$, 1.2 mM $MgCl_2$, 0.8 mM $MgSO_4$•$7H_2O$, pH 7.4), potassium buffer (135 mM KCl, 28 mM D-glucose, 13 mM HEPES, 5 mM NaCl, 2.5 mM $CaCl_2$•$2H_2O$, 1.2 mM $MgCl_2$, 0.8 mM $MgSO_4$•$7H_2O$, pH 7.4), and sulfate buffer (67.5 mM Na_2SO_4, 28 mM D-glucose, 13 mM HEPES, 2.5 mM K_2SO_4, 2.5 mM $Ca(HCO_3)_2$, 2 mM $MgSO_4$•$7H_2O$, pH 7.4) were used to assess ion dependency of H2-GMZ uptake. In some experiments, known transporter substrates or inhibitors were added to determine the transporter(s) involved in the flux of the test compound.

JPET Fast Forward. Published on July 2, 2022 as DOI: 10.1124/jpet.122.001195
This article has not been copyedited and formatted. The final version may differ from this version.

Drug transport was terminated by washing the cells with fresh, ice-cold transport buffer before preparing the samples for LC-MS/MS analysis. After termination of transport, cells were lysed overnight with 1:1 MeOH:ACN containing 500 ng/mL internal standard (IS) at 4°C. Calibration curves were generated by serial diluting each compound from 1000 to 31.25 ng/mL or higher/lower where appropriate. The R^2 for the calibration curves were 0.99 or higher when calculating unknown sample concentrations. Following lysis, samples were dried and resuspended in 2:1:1 H_2O:MeOH:ACN with 0.1% formic acid. Samples were centrifuged at 15000 x *g* for 20 min and the supernatant was collected for LC-MS/MS analysis. A Shimadzu Prominence HPLC system (Shimadzu, Kyoto, Japan) coupled to a SCIEX QTRAP 4500 mass spectrometer (SCIEX, Framingham, MA, USA) or a SCIEX QTRAP 6500 mass spectrometer (SCIEX, Framingham, MA, USA) operating in multiple reaction monitoring (MRM) mode with positive or negative ESI was used to detect intracellular accumulation of each tested compound. The source parameters for the QTRAP 4500 (or QTRAP 6500) were: 5.5 or -4.5 kV ion spray voltage, 500°C source temperature, 20 (or 45) psi nebulizer gas, 40 (or 55) psi turbo gas, 10 (or 35) psi curtain gas, and 9 (or 8) psi collision gas.

The MS parameters for MRM analysis of each compound are listed in Table 1. JWS-2-112 served as the IS for H2-GMZ, GMZ, and RC-MC-241, whereas H2-GMZ served as the IS for the JWS-2-112, JWS-2-176, and RC-MC-100. Trofosfamide served as the IS for diclofenac and indomethacin. Ten microliters of each sample were injected onto an InfinityLab Poroshell 120 EC-C18 column (3.0 x 50 mm x 2.7 µm; Agilent, Santa Clara, CA, USA, Catalog #699975-302) for LC-MS/MS analysis. The compounds were

JPET Fast Forward. Published on July 2, 2022 as DOI: 10.1124/jpet.122.001195
This article has not been copyedited and formatted. The final version may differ from this version.

eluted with a gradient elution using a mobile phase A consisting of 0.1% formic acid in H_2O and a mobile phase B consisting of 0.1% formic acid in ACN. Total sample acquisition time was 6 min with a 2 min equilibration time between each sample. Peaks were quantified using SCIEX MultiQuant software and further analyzed with Microsoft Excel and GraphPad Prism 8 (GraphPad Software, San Diego, CA, USA).

Transport Assay by Radioactive Liquid Scintillation Counting

Confluent monolayers of HEK-293-EV, HEK-293-OATP1A2, Flp-In CHO, or CHO-OATP2B1 cells cultured in 96-well plates were used to assess total [^{3}H]E3S uptake. Transport experiments were performed as previously described with minor modifications (Severance et al., 2017; Sandoval et al., 2018; Hau et al., 2020; Miller et al., 2020). Cells were plated into Nunc MicroWell 96-well optical bottom plates (ThermoFisher Scientific, Waltham, MA, USA, Catalog #165306) and grown to confluence before each experiment. Confluent cells plated were washed twice with room temperature WB before incubating wells with 50 µL WB transport buffer supplemented with 1 µCi/mL (~15-20 nM) [^{3}H]E3S with or without inhibitors. To determine the IC_{50} for transport inhibition produced by H2-GMZ, cells were plated into Nunc MicroWell 96-well optical bottom plates (ThermoFisher Scientific, Waltham, MA, USA, Catalog #165306) and grown to confluence before each experiment. Cells were washed twice with room temperature WB and transport was initiated by adding 50 µL of transport buffer containing 1 µCi/mL (~15-20 nM) [^{3}H]E3S and serially diluted H2-GMZ (0.01 – 1 mM) to the cells. Transport was terminated after 5 min by washing the cells twice with ice-cold WB using a Biotek 405 LS Microplate Washer (BioTek, Winooski,

VT, USA). After washing, approximately 200 µL of MicroScint-20 scintillation cocktail (PerkinElmer, Waltham, MA, USA, Catalog #6013621) was added to each well before sealing the plate with microplate film. Plates were incubated at room temperature for at least 2 hrs before measuring total accumulated radioactivity using a Wallac 1450 MicroBeta TriLux liquid scintillation counter (PerkinElmer, Waltham, MA, USA). Total radiolabeled signal in HEK-293-OATP1A2 or CHO-OATP2B1 cells were subtracted from their control counterparts to determine final [^{3}H]E3S uptake.

Statistical Analysis

Each experiment was completed with cells cultured from at least two separate passages with two to four replicates, as necessary. All data were analyzed using GraphPad Prism 8 (GraphPad Software, San Diego, CA, USA). An ordinary one-way ANOVA with Bonferroni's multiple comparisons correction was used to identify a statistically significant decrease in drug uptake with the transport experiments in SCs.

Transport kinetics data was fitted with the Michaelis-Menten equation plus a first-order component as defined by equation 1 (Sandoval et al., 2018; Sandoval et al., 2019; Miller et al., 2020; Miller et al., 2021), which accounts for non-saturable (non-transporter-mediated) substrate accumulation over the range of concentrations tested. In the following equations, J_{total} and J represent the initial rate of total or transporter-mediated substrate uptake, respectively, from a given concentration ([S]); $J_{max\text{-}app}$ is the apparent maximal rate of transported-mediated substrate uptake; $K_{t\text{-}app}$ indicates the apparent Michaelis constant; and K_d is a constant that describes the first-order component of total substrate uptake.

$$\text{Equation 1: } J_{total} = \frac{Jmax-app \bullet [S]}{K_{t-app} + [S]} + K_d[S]$$

To correct for the first-order component, the K_d obtained from fitting equation 1 to the data was multiplied with the tested concentration and subtracted from total uptake at that concentration. A new Michaelis-Menten equation was fitted to the corrected data as described by equation 2 to calculate the reported $J_{max\text{-}app}$ and $K_{t\text{-}app}$ values.

$$\text{Equation 2: } J = \frac{Jmax-app \bullet [S]}{K_{t-app} + [S]}$$

Kinetic parameters were calculated per experiment to obtain standard deviations. The IC_{50} values of H2-GMZ on OATP1A2- or OATP2B1-mediated [^{3}H]E3S uptake were calculated using equation 3 (Groves et al., 1994; Sandoval et al., 2018; Sandoval et al., 2019; Hau et al., 2020; Miller et al., 2021).

$$\text{Equation 3: } J = \frac{Jm-app^* \bullet [T]}{IC_{50} + [S]} + K_d[T]$$

In this equation, J represents total [^{3}H]E3S transport, $J_{m\text{-}app}$* is a constant (J_{max} for E3S multiplied by the ratio of the IC_{50} for the inhibitor and the K_t for E3S), [T] indicates the [^{3}H]E3S concentration, and [I] is the H2-GMZ concentration. The IC_{50} values for H2-GMZ inhibition of [^{3}H]E3S uptake in HEK-293-OATP1A2 or CHO-OATP2B1 cells were reported with 95% confidence intervals and an R^2 value for the goodness of fit. All data are presented as mean ± S.D unless otherwise indicated. Significance is indicated as *: $p \leq 0.05$, **: $p \leq 0.01$, ***: $p \leq 0.001$, and ****: $p \leq 0.0001$.

JPET Fast Forward. Published on July 2, 2022 as DOI: 10.1124/jpet.122.001195
This article has not been copyedited and formatted. The final version may differ from this version.

Results

Kinetics of Indazole Carboxylic Acid Analog Transport in Sertoli Cells

The concentration-dependent uptake of 5 indazole carboxylic acid analogs was assessed in hT-SerCs with additional transport experiments to evaluate concentration-dependent H2-GMZ uptake in primary rat SCs. H2-GMZ and GMZ were tested at serially diluted concentrations up to 1000 μM. Due to limitations with solubility and the maximum concentration of the stock solutions, the maximum tested concentrations were 150 μM for JWS-2-112, RC-MC-100, and RC-MC-241 and 100 μM for JWS-2-176. H2-GMZ displayed concentration-dependent saturability in hT-SerCs and rat SCs, which is indicative of Michaelis-Menten transport kinetics. The $J_{max\text{-}app}$ for H2-GMZ was 266 ± 112 and 259 ± 62.9 pmol/cm^2•min in hT-SerCs and rat SCs, respectively (Figures 1A and 1B). Correspondingly, the $K_{t\text{-}app}$ for H2-GMZ were also similar at 138 ± 39.3 and 151 ± 43.2 μM in hT-SerCs and rat SCs (Figures 1A and 1B), indicating there may be shared transport pathways for this compound between species.

Transport of GMZ, JWS-2-112, RC-MC-100, and RC-MC-241 into hT-SerCs also exhibited typical Michaelis-Menten kinetics with saturability evident at higher concentrations (Figures 2A, B, D, and E), whereas JWS-2-176 did not appear to

JPET Fast Forward. Published on July 2, 2022 as DOI: 10.1124/jpet.122.001195
This article has not been copyedited and formatted. The final version may differ from this version.

effectively penetrate hT-SerCs over the range of concentrations examined (Figure 2C). The $J_{max\text{-}app}$ for GMZ was 232 ± 56.5 pmol/cm^2•min and the $K_{t\text{-}app}$ was 38.3 ± 1.28 μM in hT-SerCs (Figure 2A). Unlike JWS-2-176, the $J_{max\text{-}app}$ for JWS-2-112 was 283 ± 80.2 pmol/cm^2•min and the $K_{t\text{-}app}$ was 48.0 ± 1.32 μM in hT-SerCs (Figure 2B). The $J_{max\text{-}app}$ for RC-MC-100 and RC-MC-241 was slightly lower than the other analogs at 197 ± 15.1 and 179 ± 39.5 pmol/cm^2•min and the $K_{t\text{-}app}$ were 83.0 ± 30.6 and 25.5 ± 6.03 μM, respectively (Figures 2D and 2E). A summary of kinetic parameters for each drug is listed in Table 2.

Inhibition of H2-GMZ Uptake into hT-SerCs

In an effort to identify the transporter(s) involved in the uptake of H2-GMZ into hT-SerCs, a structurally diverse battery of potentially competitive substrates and inhibitors were co-incubated with 30 μM H2-GMZ for 5 min (Figure 3A). After termination of transport, total accumulation of H2-GMZ was measured in hT-SerCs by LC-MS/MS. Several compounds inhibited H2-GMZ uptake with statistically significant decreases as indicated by the red bars. Whereas substrates and inhibitors of the ENTs, CNTs, OATs, OCTs, and OCTNs had little to no effect on H2-GMZ uptake, 500 μM T3 hormone and 1 mM lithocholic acid, which are typical substrates of some OATPs, elicited a ~40-50% reduction in H2-GMZ uptake (Figure 3A). However, other OATP substrates, including fluorescein, E3S, and taurocholic acid exerted minimal effects on H2-GMZ uptake (Figure 3A).

Although many compounds had minimal effect on H2-GMZ uptake in hT-SerCs, 1 mM indomethacin, diclofenac, and MK-571 inhibited uptake by 54%, 58%, and 79%,

JPET Fast Forward. Published on July 2, 2022 as DOI: 10.1124/jpet.122.001195
This article has not been copyedited and formatted. The final version may differ from this version.

respectively (Figure 3B). In separate studies, indomethacin and diclofenac were also found to be transported into hT-SerCs and rat SCs in a concentration dependent manner. The $J_{max\text{-}app}$ values for indomethacin in hT-SerCs and rat SCs were 46.1 ± 17.4 and 46.5 ± 0.42 pmol/cm^2•min, and the $K_{t\text{-}app}$ were 62.2 ± 13.2 and 67.2 ± 13.9 μM, respectively (Figure S1A and S1B). Several compounds inhibited indomethacin uptake into hT-SerCs, with H2-GMZ (150 μM), diclofenac, MK-571, bromsulphthalein, and repaglinide (each at 1 mM) exerting the greatest reduction of indomethacin uptake (Figure S3A).

Likewise, in hT-SerCs and rat SCs, the $J_{max\text{-}app}$ for diclofenac was 56.6 ± 17.3 and 75.5 ± 7.50 pmol/cm^2•min, with $K_{t\text{-}app}$ values of 80.1 ± 56.3 and 112 ± 11.1 μM, respectively (Figure S2A and S2B). A summary of kinetic values for indomethacin and diclofenac are listed in Table S1. Uptake of diclofenac into hT-SerCs was also inhibited by 150 μM H2-GMZ, 1 mM indomethacin, 1 mM MK-571, and 1 mM repaglinide (Figure S3A and S3B). In contrast, 1 mM bromsulphthalein, lithocholic acid, probenecid, and 5 mM pyruvic acid did not elicit statistically significant reductions to diclofenac uptake, compared to indomethacin uptake (Figure S3A and S3B). Other tested compounds shared similar non-inhibitory profiles against indomethacin or diclofenac uptake. Most importantly, the inhibition of indomethacin and diclofenac uptake by H2-GMZ suggests these three compounds share at least one transport pathway into hT-SerCs, although there may be other uptake pathways for indomethacin.

In separate transport experiments with hT-SerCs, several indazole carboxylic acid analogs were co-incubated with H2-GMZ to determine their inhibitory effects. Co-incubation with JWS-2-112, RC-MC-100, and RC-MC-241 caused statistically significant

decreases to H2-GMZ uptake (Figure 3C). RC-MC-100 and RC-MC-241 were able to inhibit H2-GMZ uptake by >50%, with JWS-2-112 only decreasing uptake by ~30% at the tested concentrations. Interestingly, JWS-2-176 and Adjudin did not exert a significant inhibitory effect against H2-GMZ uptake.

Role of Extracellular Ion Levels in H2-GMZ Transport

The impact of extracellular ions, including H^+, Na^+, K^+, and Cl^-, was investigated to further characterize the transporter-mediated processes involved in the uptake of H2-GMZ into hT-SerCs. A series of standardized transport buffers at pH values ranging from 6.5 to 8.0 were tested to identify a pH-dependent mechanism of transport. With an extracellular pH of 6.5, uptake of H2-GMZ into hT-SerCs was stimulated by ~34% compared to the control physiological pH 7.4 (Figure 4A). Inversely, uptake of H2-GMZ into hT-SerCs was significantly reduced by ~41% at pH 8.0 (Figure 4A). Uptake of H2-GMZ followed an increasing trend at pH 7.0 and a decreasing trend at pH 7.5 but were not statistically significant.

To assess the effects of extracellular Na^+ on H2-GMZ uptake, choline buffer, which replaced all Na^+ with choline ions, was used. Compared to the standard transport buffer (control), there was no statistically significant change in H2-GMZ uptake indicating any major H2-GMZ transport processes were independent of Na^+ levels (Figure 4B). Potassium transport buffer containing a low Na^+ concentration (5 mM) and high K^+ concentration (135 mM) was used to assess the impact of high K^+ levels. Likewise, transporter-mediated uptake of H2-GMZ was not changed by high K^+ levels (Figure 4B). Lastly, sulfate buffer, which completely replaced all Cl^- with SO_4^{2-} or OH^-

JPET Fast Forward. Published on July 2, 2022 as DOI: 10.1124/jpet.122.001195
This article has not been copyedited and formatted. The final version may differ from this version.

was used to evaluate the role of Cl^- in H2-GMZ uptake. Like other ions, extracellular Cl^- levels had no effect on H2-GMZ uptake into hT-SerCs (Figure 4B).

Kinetics and Inhibition of H2-GMZ Uptake into Native CHO, MDCK, and HEK-293 Cells

The transport kinetics of H2-GMZ was evaluated in native CHO, MDCK, and HEK-293 cells to identify an ideal cell line for subsequent heterologous transporter overexpression studies. All three native cell lines exhibited greater capacity for H2-GMZ transport than hT-SerCs over the range of concentrations tested. The $J_{max\text{-}app}$ for H2-GMZ in CHO, MDCK, and HEK-293 cells was 804 ± 108, 1040 ± 384, and 2810 ± 613 pmol/cm^2•min, respectively (Figures 5A-C). The $K_{t\text{-}app}$ was 160 ± 28.1, 121 ± 57.6, and 472 ± 153 μM in CHO, MDCK, and HEK-293 cells (Figures 5A-C). The $K_{t\text{-}app}$ of H2-GMZ in CHO and MDCK cells were similar to that observed in hT-SerCs; however, the $J_{max\text{-}app}$ in all three of the native cell lines was 3- to 4-fold greater. Interestingly, there was no significant first-order component to subtract from the uncorrected H2-GMZ kinetic data in HEK-293 cells. A summary of kinetic values for H2-GMZ in each cell line are listed in Table 2.

The inhibitory effects of indomethacin, diclofenac, and MK-571 against H2-GMZ uptake were assessed in each of the three native cell lines. Notably, 1 mM diclofenac and MK-571 elicited a statistically significant decrease in H2-GMZ uptake in all three cell lines (Figure 5D). Indomethacin caused a statistically significant decrease in H2-GMZ uptake in CHO and HEK-293 cells; uptake in MDCK cells showed a similar trend, though it did reach statistical significance (Figure 5D). Importantly, indomethacin, diclofenac, and MK-571 inhibition of H2-GMZ uptake was less potent in the native cells

compared to hT-SerCs, suggesting other distinct pathways dominate H2-GMZ uptake in these cell lines, making them effectively unsuitable for additional studies.

H2-GMZ Interaction with Human OATP1A2 and OATP2B1

Based on previous reports on the expression of OATPs at the BTB (Hau et al., 2022) and the interactions between H2-GMZ and human OATPs (Shoop et al., 2014), the interaction between H2-GMZ and human OATP1A2 or OATP2B1 was evaluated. Membrane expression of human OATP1A2 or OATP2B1 was confirmed by immunocytofluorescence with an anti-Flag or anti-V5 antibody, respectively. Expression of the Flag-tagged OATP1A2 was observed throughout the cytoplasm and at the plasma membrane of HEK-293 cells (Figure S4B), and V5-tagged OATP2B1 displayed a similar expression profile in Flp-In CHO cells (Figure S4D).

Uptake of the prototypical substrate, [^{3}H]E3S, was also measured to confirm functional expression of OATP1A2 or OATP2B1 at the membrane in each cell line compared to their control counterparts. Both overexpressing cell lines exhibited significantly higher uptake of [^{3}H]E3S compared to control cells, which was negligible. These findings confirmed functional expression of OATP1A2 or OATP2B1 at the plasma membrane of each cell line, despite exhibiting some cytoplasmic staining with the immunolocalization assay (Figures S4B and S4D). As a result, the background radiolabeled [^{3}H]E3S signal measured in control cells were subtracted from the values obtained from HEK-293-OATP1A2 or CHO-OATP2B1 cells to resolve specific human OATP1A2- or OATP2B1-mediated uptake. Uptake of [^{3}H]E3S mediated by both OATP1A2 and OATP1B1 was inhibited by H2-GMZ in a concentration dependent

manner at physiological pH 7.4 (Figures 6A and 6B). The IC_{50} values for H2-GMZ was 20.6 (95% CI: 12.6, 34.1) and 93.7 μM (95% CI: 62.7, 141) in CHO-OATP2B1 and HEK-293-OATP1A2 cells, respectively.

Due to previous studies reporting that OATP-mediated transport is pH-sensitive (Kobayashi et al., 2003; Nozawa et al., 2004; Leuthold et al., 2009; Patik et al., 2015; Sato et al., 2021) and H2-GMZ uptake in hT-SerCs exhibiting that characteristic in this study (Figure 3A), the dynamic inhibitory effect of H2-GMZ at an acidic pH (6.0) of OATP1A2- and OATP2B1-mediated [^{3}H]E3S transport was evaluated. At pH 6.0, the rate of uptake of [^{3}H]E3S in the absence of an inhibitor increased by 2.5-fold in CHO-OATP2B1 and 1.7-fold in HEK-293-OATP1A2 cells compared to control cells, and the IC_{50} values for H2-GMZ in CHO-OATP2B1 and HEK-293-OATP1A2 cells shifted to the right to 51.6 (95% CI: 33.8, 80.2) and 155.3 μM (95% CI: 117, 207), respectively (Figures 6C and 6D). The R^2 values for the goodness of fit for the [^{3}H]E3S inhibition experiments ranged from 0.841 to 0.958 (Figures 6A-D).

Due to the inhibitory interaction observed between H2-GMZ and OATP1A2/OATP2B1, transport assays with subsequent LC-MS/MS analysis to directly measure H2-GMZ in HEK-293-EV, HEK-293-OATP1A2, Flp-In CHO, and CHO-OATP2B1 cells were performed. No discernible increase in H2-GMZ uptake was observed in HEK-293-OATP1A2 or CHO-OATP2B1 cells compared to their control counterparts (Figure 6E and 6F). Consequently, endogenous transporters expressed in these two cell lines appeared to dominate H2-GMZ uptake as observed previously (Figure 5A and 5C) and further investigation with these cell lines was abandoned.

JPET Fast Forward. Published on July 2, 2022 as DOI: 10.1124/jpet.122.001195
This article has not been copyedited and formatted. The final version may differ from this version.

Discussion

H2-GMZ was developed as a potent, non-hormonal, and reversible male contraceptive based on structure-activity relationship studies with existing indazole carboxylic acid scaffolds. Rats treated with a single 3 or 6 mg/kg dose of H2-GMZ exhibited more than 10 times greater testes-specific accumulation compared to the liver, lungs, kidneys, and the heart after 24 hours, as well as decreased testis weight and spermatogenic index after 5 days postdose (Gupta et al., 2011; Shoop et al., 2014). Furthermore, H2-GMZ interacts with intracellular proteins such as HSP90, like its analog, GMZ (Tash et al., 2008b; Sundar et al., 2020). Despite these observations, the mechanism of entry for H2-GMZ and other analogs into cells has not been identified. In this study, the physiological characteristics of H2-GMZ transport into SCs and other epithelial cell lines is described, with the primary focus on the human uptake transporters that are involved due to the potential issues studying rodent transporters outlined above.

H2-GMZ uptake in hT-SerCs and primary rat SCs exhibited concentration-dependent saturability over a range of concentrations up to 1000 μM (Figures 1A and 1B), which is indicative of typical Michaelis-Menten transport kinetics. The first-order

component, attributed to non-specific binding and incomplete rinsing of the substrate-containing buffer, was subtracted from the uncorrected data to generate the corrected data. The similar $K_{t\text{-}app}$ values between human and rat SCs suggests that H2-GMZ may share the same transport pathways between species, although further work would be required to identify the orthologs involved. Shared transport pathways for H2-GMZ are important to establish the clinical relevance of rodent models because the expression, localization, selectivity, and kinetics of some transporters are inconsistent between species (Chu et al., 2013; Hau et al., 2021). Although there may be differences in transporter expression and selectivity between hT-SerCs and primary rat SCs, the similar kinetic profile for H2-GMZ uptake is promising for clinical translatability of rodent data.

Although JWS-2-112, JWS-2-176, RC-MC-100, and RC-MC-241 did not elicit a contraceptive effect in rats (unpublished data), the transport kinetics of GMZ, JWS-2-112, JWS-2-176, RC-MC-100, and RC-MC-241 into hT-SerCs were evaluated. GMZ, JWS-2-112, RC-MC-100, and RC-MC-241 exhibited Michaelis-Menten kinetics of transport; however, despite its structural similarity to the transported congeners, JWS-2-176 did not appear to penetrate into hT-SerCs (Figures 2A-E). Inhibition experiments revealed that JWS-2-112, RC-MC-100, and RC-MC-241 inhibited H2-GMZ uptake into hT-SerCs, whereas JWS-2-176 and Adjudin had negligible effects. The lack of H2-GMZ inhibition by JWS-2-176 is consistent with its status as a non-transported compound. Additionally, these observations suggest that, although Adjudin is transported into cells by rat OCTN2, OATP1A5, OATP6B1, and OATP6C1 (Su et al., 2011), it does not share principal transport pathways with H2-GMZ in hT-SerCs. It is possible that higher

concentrations of JWS-2-176 and Adjudin exert a greater inhibitory effect on H2-GMZ uptake; however, solubility limitations prohibited further testing and the higher concentrations required to inhibit H2-GMZ uptake implies that these compounds have very different kinetic profiles. The inhibition of H2-GMZ uptake by some analogs, but not others, strongly suggests that the transport pathway(s) is(are) selective for certain structural features of these compounds despite some demonstrating pharmacological inactivity.

To help identify the transporters that are involved in H2-GMZ transport in hT-SerCs, an assortment of transporter substrates or inhibitors were co-incubated with H2-GMZ. Most compounds had no effect on H2-GMZ accumulation, although there were several that elicited a >50% decrease. Compounds that caused non-statistically significant, <30% reductions, included substrates or inhibitors of the ENTs (uridine, NBMPR), CNTs (uridine), OATs (PAH, cGMP), OCTs (cimetidine, metformin, MPP^+), OCTNs (ergothioneine, carnitine, verapamil), P-gp (ketoconazole, quercetin, verapamil, dexamethasone, clotrimazole), and BCRP (quercetin, taurocholic acid, dexamethasone). None of the tested compounds caused a statistically significant increase in H2-GMZ uptake, suggesting that transporter-mediated uptake outweighs efflux and/or H2-GMZ is not a substrate of BTB efflux transporters. Furthermore, the testes-specific accumulation of H2-GMZ *in vivo* suggests that BTB efflux transporters are unlikely to influence net disposition across the BTB. The compounds that elicited a statistically significant decrease in H2-GMZ uptake included ketoconazole, T3 hormone, lithocholic acid, bromsulphthalein, and probenecid at the indicated concentrations. Notably, indomethacin, diclofenac, and MK-571 elicited the largest decrease in H2-GMZ

uptake. MK-571 is a broad-spectrum inhibitor of many transporters including P-gp, MRPs, OATs, and OATPs (Letschert et al., 2006; Badagnani and Monshouwer, 2008; Matsson et al., 2009; Karlgren et al., 2012b; Henjakovic et al., 2015). The greater inhibitory effect of MK-571 on H2-GMZ uptake suggests that more than one pathway may be involved that are not equally shared between H2-GMZ, indomethacin, and diclofenac. Indomethacin and diclofenac are both NSAIDs with broad interactivity as substrates and allosteric inhibitors of various transporters, including the OATPs (Draper et al., 1997; Kouzuki et al., 2000; Khamdang et al., 2002; Shitara et al., 2002; El-Sheikh et al., 2007; Westholm et al., 2009; Karlgren et al., 2012a). There is also contrasting evidence that indomethacin and diclofenac exert therapeutic or toxic effects on spermatogenesis (Abbatiello et al., 1975; Moskovitz et al., 1987; Othman et al., 2001; Mogilner et al., 2006; Arslan et al., 2016; Vyas et al., 2019). Despite these contradictory observations, these two compounds may share an important BTB transport pathway. Further assessment of these two compounds revealed that both are transported into hT-SerCs and primary rat SCs in a concentration-dependent manner (Figures S1A, S1B, S2A, and S2B). Moreover, indomethacin or diclofenac uptake into hT-SerCs was significantly inhibited by H2-GMZ and MK-571 (Figures S3A and S3B). Therefore, H2-GMZ, indomethacin, and diclofenac may share at least one transport pathway into hT-SerCs; however, further studies are necessary to identify these shared transporters and others specifically involved in H2-GMZ transport.

Inhibition experiments revealed common OATP substrates or inhibitors, such as indomethacin, diclofenac, MK-571, T3 hormone, and lithocholic acid, generally had the largest inhibitory effect on H2-GMZ uptake. However, other OATP substrates (E3S,

taurocholic acid, and fluorescein) were less effective. These differences may be attributed to multiple OATPs or unknown transporters involved in the uptake of H2-GMZ, wherein other transporters can compensate if one transporter is compromised. The broad-spectrum activity of indomethacin, diclofenac, and MK-571 on the OATPs lends credence to this hypothesis, although it does not offer a complete explanation for these observations. Therefore, the characteristics of H2-GMZ transport were further defined by modifying ion concentrations in the transport buffer. Uptake of H2-GMZ at pH 6.5 was significantly increased in hT-SerCs compared to physiological pH 7.4 (Figure 4A). Furthermore, uptake at pH 8.0 was markedly decreased (Figure 4A), indicating a transporter-mediated dependence on extracellular H^+ levels. The predicted pK_a (4.33) of H2-GMZ suggests that there are nearly 150-fold more ionized molecules of H2-GMZ at pH 6.5, which opposes the conclusion that passive diffusion is responsible for the observed increase. Moreover, H2-GMZ uptake was independent of extracellular Na^+, K^+, and Cl^- levels in hT-SerCs at pH 7.4 (Figure 4B). This ion-independent, pH-sensitive phenomenon is commonly associated with OATP-mediated transport (Satlin et al., 1997; Kobayashi et al., 2003; Hagenbuch and Meier, 2004; Hagenbuch and Gui, 2008; Leuthold et al., 2009; Roth et al., 2012; Patik et al., 2015; Sato et al., 2021). Consequently, further studies correlating the interaction between H2-GMZ and OATPs were performed.

Conventional cell lines including CHO, MDCK, and HEK-293 cells have been used to overexpress OATPs; however, they also express many endogenous transporters (Goh et al., 2002; Ahlin et al., 2009). H2-GMZ uptake was measured in CHO, MDCK, and HEK-293 cells to identify an appropriate cell line for heterologous

transporter overexpression studies. Each of the cell lines exhibited greater capacity for H2-GMZ uptake as shown by the 3- to 4-fold greater $J_{max\text{-}app}$ compared to hT-SerCs, with CHO and MDCK cells exhibiting similar rates of transport ($K_{t\text{-}app}$) as in hT-SerCs, despite expressing orthologous transporters. HEK-293 cells had a 3-fold greater $K_{t\text{-}app}$ than all other cells, suggesting that there may be high functional expression of one or more human transporters for H2-GMZ. Notably, there was no significant first-order component to subtract from the uncorrected data when analyzing the transport kinetics of H2-GMZ in HEK-293 cells compared to other tested cells. Since the K_d of is calculated based on the raw data and curve-fitting, a low K_d will not contribute to a significant first-order component at high substrate concentrations. This discrepancy is likely due to the extra precautions taken when working with the physically sensitive HEK-293 cells and mathematically correcting the data based on equation 1. However, the effect of indomethacin, diclofenac, and MK-571 on H2-GMZ uptake in each cell line was also tested and revealed varying degrees of inhibition that is attributed to transporter-mediated uptake. As expected, the total amount of H2-GMZ was higher in all cell lines compared to hT-SerCs, although the effect of the three inhibitory compounds was also lower (Figures 3B and 5D). This observation suggests that there are multiple processes capable of supporting H2-GMZ transport, some of which are not affected by these broad-spectrum transport inhibitors. However, the processes capable of supporting H2-GMZ transport in these cell lines will have to be identified in future studies.

A previous study noted that H2-GMZ inhibited uptake of estradiol-17β-glucuronide, E3S, taurocholate, and pravastatin in CHO-OATP1B1 and CHO-OATP1B3

cells; however, direct uptake of [^{3}H]H2-GMZ was not observed (Shoop et al., 2014). Moreover, expression of OATP1A2, OATP2B1, and others have been observed in at the basal membrane of human SCs (Hau et al., 2022). Therefore, the role of OATP1A2 and OATP2B1 in H2-GMZ uptake was assessed. H2-GMZ inhibited OATP1A2- and OATP2B1-mediated uptake of [^{3}H]E3S in a concentration dependent manner. [^{3}H]E3S uptake by OATP1A2 or OATP2B1 was pH-dependent and the IC_{50} for H2-GMZ inhibition was increased by ~1.7–2.5-fold at pH 6.0 versus pH 7.4 (Figures 6A-D). Although H2-GMZ inhibited OATP1A2- and OATP2B1-mediated uptake, there was no discernible increase in uptake when directly measured in HEK-293-OATP1A2 or CHO-OATP2B1 cells compared to control cells at pH 7.4 by LC-MS/MS analysis (Figures 6E and 6F). The contribution of OATP1A2- or OATP2B1-mediated uptake of H2-GMZ was minimal compared to endogenous transporters. Although 1 mM MK-571 could inhibit total H2-GMZ uptake by ~56% and ~40% in CHO and HEK-293 cells, respectively, the remaining signal may be attributed to endogenous transporters that do not interact with MK-571 or is due to non-specific binding or incomplete rinsing of the substrate-containing buffer. Identifying the contribution of each transporter-mediated process would require future studies using single or multiple transporter knockout or knockdown cell lines.

It is also possible that there are transport pathways for H2-GMZ that differ from known transporters that have been functionally characterized to date. Early studies functionally characterized novel transporters for endogenous and exogenous chemicals before the genes were formally identified. These studies observed notable differences in tissue expression levels and the initial rates of uptake and K_t values between rodent

OATP1 and the cloned human OATP despite similar substrate selectivity (Kullak-Ublick et al., 1995; Bossuyt et al., 1996; Meier et al., 1997), suggesting the existence of the then-unknown, human liver-specific transporter 1 (also known as OATP1B1) (Abe et al., 1999). Similarly, the functional transport characteristics of a sodium-dependent bile acid transporter were well-defined (Berk et al., 1987; Frimmer and Ziegler, 1988; Zimmerli et al., 1989) before molecular cloning experiments led to the identification of the sodium-taurocholate co-transporting polypeptide gene (Hagenbuch et al., 1991; Hagenbuch and Meier, 1994). There are hundreds of transporters that have been identified through whole genome analysis; however, many of them are not as well-characterized as the transporters of significant clinical importance as recommended by the U.S. Food and Drug Administration and International Transporter Consortium (Giacomini et al., 2018; FDA, 2020a; FDA, 2020b; Zamek-Gliszczynski et al., 2022). For example, OATP6A1 is known to be highly and specifically expressed in the testes and in certain cancers (Suzuki et al., 2003; Lee et al., 2004; Fietz et al., 2013); however, it has yet to be functionally characterized in heterologous expression systems like OATP1B1 or OATP1B3 despite previous attempts (unpublished data). It is conceivable that H2-GMZ is a substrate of OATP6A1 due to its specific expression in the testes, although current technologies limit these functional transport studies. Consequently, an extensive transporter knockout screening study that includes these understudied transporters may be necessary to identify the specific transporter(s) involved in H2-GMZ uptake.

In summary, this study is the first to characterize the transport of the experimental contraceptive, H2-GMZ, across cell membranes. The data presented here shows that multiple transporters are involved in the transport of H2-GMZ, but at least

one pathway exhibits the pH-sensitive and ion-independent characteristics of OATP-mediated transport. One or more unknown transporters may share these characteristics with the OATPs, but future studies that knockout or knockdown single or multiple endogenous transporters will be necessary. Multiple transporter knockout or knockdown models may be necessary to account for other transporters that compensate for the transporters that have loss of function. Nevertheless, these findings provide insight into the mechanism(s) by which H2-GMZ, relevant analogs, and other compounds can bypass the BTB and exert their pharmacological effect.

Acknowledgements

We thank Dr. James Galligan of the Department of Pharmacology & Toxicology at the University of Arizona (Tucson, AZ, USA) for his help and knowledge on using the LC-MS/MS. The authors thank Dr. Bruno Stieger and Stephanie Bernhard of the Department of Clinical Pharmacology and Toxicology at the University of Zurich (Zürich, Switzerland) for providing several human OATP gene inserts for this study. We would also like to thank Dr. Bruno Hagenbuch of the Department of Pharmacology, Toxicology & Therapeutics at the University of Kansas Medical Center (Kansas City, Kansas, USA) for providing the HEK-293-EV and HEK-293-OATP1A2 cells used in this study. We also thank Alan Yu, Carolyn Vivian, and Melinda Broward at University of Kansas Medical

Center (Kansas City, Kansas, USA) for storing and providing the indazole carboxylic acid analogs used in this study that were synthesized by Drs. Sudhakar Jakkaraj and Ramappa Chakrasali.

Authorship Contributions

Participated in research design: Hau, Tash, Georg, Wright, and Cherrington

Conducted experiments: Hau

Contributed new reagents or analytical tools: Tash and Georg

Performed data analysis: Hau, Tash, Georg, Wright, and Cherrington

Wrote or contributed to the writing of the manuscript: Hau, Tash, Georg, Wright, and Cherrington

References

Abbatiello ER, Kaminsky M and Weisbroth S (1975) The effect of prostaglandins and prostaglandin inhibitors on spermatogenesis. *Int J Fertil* **20**:177-182.

Abe T, Kakyo M, Tokui T, Nakagomi R, Nishio T, Nakai D, Nomura H, Unno M, Suzuki M, Naitoh T, Matsuno S and Yawo H (1999) Identification of a novel gene family encoding human liver-specific organic anion transporter LST-1. *J Biol Chem* **274**:17159-17163.

Ahlin G, Hilgendorf C, Karlsson J, Szigyarto CA, Uhlen M and Artursson P (2009) Endogenous gene and protein expression of drug-transporting proteins in cell

lines routinely used in drug discovery programs. *Drug Metab Dispos* **37**:2275-2283.

Arslan H, Aktas A, Elibol E, Esener OB, Turkmen AP, Yurt KK, Onger ME, Altunkaynak BZ and Kaplan S (2016) Effects of prenatal diclofenac sodium exposure on newborn testis: a histomorphometric study. *Biotech Histochem* **91**:277-282.

Badagnani I and Monshouwer M (2008) *Are the commonly used drug transport inhibitors, elacridar, MK-571, and Ko143, as selective as often assumed?*

Berk PD, Potter BJ and Stremmel W (1987) Role of plasma membrane ligand-binding proteins in the hepatocellular uptake of albumin-bound organic anions. *Hepatology* **7**:165-176.

Bernie AM, Osterberg EC, Stahl PJ, Ramasamy R and Goldstein M (2012) Vasectomy reversal in humans. *Spermatogenesis* **2**:273-278.

Bossuyt X, Muller M and Meier PJ (1996) Multispecific amphipathic substrate transport by an organic anion transporter of human liver. *J Hepatol* **25**:733-738.

Chao J, Page ST and Anderson RA (2014) Male contraception. *Best Pract Res Clin Obstet Gynaecol* **28**:845-857.

Chao JH and Page ST (2016) The current state of male hormonal contraception. *Pharmacol Ther* **163**:109-117.

Cheng CY, Mruk D, Silvestrini B, Bonanomi M, Wong CH, Siu MK, Lee NP, Lui WY and Mo MY (2005) AF-2364 [1-(2,4-dichlorobenzyl)-1H-indazole-3-carbohydrazide] is a potential male contraceptive: a review of recent data. *Contraception* **72**:251-261.

Chu X, Bleasby K and Evers R (2013) Species differences in drug transporters and implications for translating preclinical findings to humans. *Expert Opin Drug Metab Toxicol* **9**:237-252.

Coulston F, Dougherty WJ, LeFevre R, Abraham R and Silvestrini B (1975) Reversible inhibition of spermatogenesis in rats and monkeys with a new class of indazol-carboxylic acids. *Exp Mol Pathol* **23**:357-366.

De Martino C, Malcorni W, Bellocci M, Floridi A and Marcante ML (1981) Effects of AF 1312 TS and lonidamine on mammalian testis. A morphological study. *Chemotherapy* **27 Suppl 2**:27-42.

Draper MP, Martell RL and Levy SB (1997) Indomethacin-mediated reversal of multidrug resistance and drug efflux in human and murine cell lines overexpressing MRP, but not P-glycoprotein. *Br J Cancer* **75**:810-815.

Dym M and Fawcett DW (1970) The blood-testis barrier in the rat and the physiological compartmentation of the seminiferous epithelium. *Biol Reprod* **3**:308-326.

El-Sheikh AA, van den Heuvel JJ, Koenderink JB and Russel FG (2007) Interaction of nonsteroidal anti-inflammatory drugs with multidrug resistance protein (MRP) 2/ABCC2- and MRP4/ABCC4-mediated methotrexate transport. *J Pharmacol Exp Ther* **320**:229-235.

Clinical Drug Interaction Studies — Cytochrome P450 Enzyme- and Transporter-Mediated Drug Interactions Guidance for Industry. U.S. Food and Drug Administration. https://www.fda.gov/regulatory-information/search-fda-guidance-documents/clinical-drug-interaction-studies-cytochrome-p450-enzyme-and-transporter-mediated-drug-interactions. Accessed 6 May 2022.

In Vitro Drug Interaction Studies — Cytochrome P450 Enzyme- and Transporter-Mediated Drug Interactions Guidance for Industry. U.S. Food and Drug Administration. https://www.fda.gov/regulatory-information/search-fda-guidance-documents/in-vitro-drug-interaction-studies-cytochrome-p450-enzyme-and-transporter-mediated-drug-interactions. Accessed 6 May 2022.

Fietz D, Bakhaus K, Wapelhorst B, Grosser G, Gunther S, Alber J, Doring B, Kliesch S, Weidner W, Galuska CE, Hartmann MF, Wudy SA, Bergmann M and Geyer J (2013) Membrane transporters for sulfated steroids in the human testis--cellular localization, expression pattern and functional analysis. *PLoS One* **8**:e62638.

Frimmer M and Ziegler K (1988) The transport of bile acids in liver cells. *Biochim Biophys Acta* **947**:75-99.

Gatto MT, Tita B, Artico M and Saso L (2002) Recent studies on lonidamine, the lead compound of the antispermatogenic indazol-carboxylic acids. *Contraception* **65**:277-278.

Gava G and Meriggiola MC (2019) Update on male hormonal contraception. *Ther Adv Endocrinol Metab* **10**:2042018819834846.

Georg GI, Tash JS, Chakrasali R and Jakkaraj SR (2010) Lonidamine analogues and their use in male contraception and cancer treatment, in, University of Kansas, University of Kansas Medical Center, United States of America.

Georg GI, Tash JS, Chakrasali R and Jakkaraj SR (2015) Lonidamine analogues and their use in male contraception and cancer treatment, in, University of Kansas, University of Kansas Medical Center, Canada.

Georg GI, Tash JS, Chakrasali R, Jakkaraj SR and Calvet JP (2013) Lonidamine analogues and treatment of polycystic kidney disease, in, University of Kansas, United States of America.

Giacomini KM, Galetin A and Huang SM (2018) The International Transporter Consortium: Summarizing Advances in the Role of Transporters in Drug Development. *Clin Pharmacol Ther* **104**:766-771.

Goh LB, Spears KJ, Yao D, Ayrton A, Morgan P, Roland Wolf C and Friedberg T (2002) Endogenous drug transporters in in vitro and in vivo models for the prediction of drug disposition in man. *Biochem Pharmacol* **64**:1569-1578.

Grima J, Silvestrini B and Cheng CY (2001) Reversible inhibition of spermatogenesis in rats using a new male contraceptive, 1-(2,4-dichlorobenzyl)-indazole-3-carbohydrazide. *Biol Reprod* **64**:1500-1508.

Groves CE, Evans KK, Dantzler WH and Wright SH (1994) Peritubular organic cation transport in isolated rabbit proximal tubules. *Am J Physiol* **266**:F450-458.

Gupta VG, Zelinski M, Steinmetz K, Miklos A, Broward M, Jakkaraj S, Chakrasali R, Georg GI and Tash JS (2011) Anti-spermatogenic efficacy of nonhormonal male contraceptive agent, H2-gamendazole, in mice, rats, rabbits, and nonhuman primates (rhesus), and a multiple low dose oral regimen that gives 100% infertility with complete reversibility. *Biology of Reproduction* **85**:5-5.

Hagenbuch B and Gui C (2008) Xenobiotic transporters of the human organic anion transporting polypeptides (OATP) family. *Xenobiotica* **38**:778-801.

Hagenbuch B and Meier PJ (1994) Molecular cloning, chromosomal localization, and functional characterization of a human liver Na+/bile acid cotransporter. *J Clin Invest* **93**:1326-1331.

Hagenbuch B and Meier PJ (2004) Organic anion transporting polypeptides of the OATP/ SLC21 family: phylogenetic classification as OATP/ SLCO superfamily, new nomenclature and molecular/functional properties. *Pflugers Arch* **447**:653-665.

Hagenbuch B, Stieger B, Foguet M, Lubbert H and Meier PJ (1991) Functional expression cloning and characterization of the hepatocyte Na+/bile acid cotransport system. *Proc Natl Acad Sci U S A* **88**:10629-10633.

Hau RK, Klein RR, Wright SH and Cherrington NJ (2022) Localization of Xenobiotic Transporters Expressed at the Human Blood-Testis Barrier. *Drug Metab Dispos*.

Hau RK, Miller SR and Cherrington NJ (2021) Implications of species differences in function and localization of transporters at the blood-testis barrier. *Toxicol Sci* **181**:1-2.

Hau RK, Miller SR, Wright SH and Cherrington NJ (2020) Generation of a hTERT-Immortalized human Sertoli cell model to study transporter dynamics at the blood-testis barrier. *Pharmaceutics* **12**.

Henjakovic M, Hagos Y, Krick W, Burckhardt G and Burckhardt BC (2015) Human organic anion transporter 2 is distinct from organic anion transporters 1 and 3 with respect to transport function. *Am J Physiol Renal Physiol* **309**:F843-851.

Heywood R, James RW, Barcellona PS, Campana A and Cioli V (1981) Toxicological studies on 1-substituted-indazole-3-carboxylic acids. *Chemotherapy* **27 Suppl 2**:91-97.

Holets LM, Cottita J, Jakkaraj S, Chakrasali R, Kinzy T, Georg G and Tash J (2011) Effect of H2-Gamendazole and Other Indazole Carboxylic Acid (ICA) Analogs on Primary Rat Sertoli Cells Cytoskeletal Structure and Elongation Factor 1 Alpha (EEF1A1) Expression and Function. *Biology of Reproduction* **85**:582-582.

Hotchkiss AG, Berrigan L and Pelis RM (2015) Organic anion transporter 2 transcript variant 1 shows broad ligand selectivity when expressed in multiple cell lines. *Front Pharmacol* **6**:216.

Karlgren M, Ahlin G, Bergstrom CA, Svensson R, Palm J and Artursson P (2012a) In vitro and in silico strategies to identify OATP1B1 inhibitors and predict clinical drug-drug interactions. *Pharm Res* **29**:411-426.

Karlgren M, Vildhede A, Norinder U, Wisniewski JR, Kimoto E, Lai Y, Haglund U and Artursson P (2012b) Classification of inhibitors of hepatic organic anion transporting polypeptides (OATPs): influence of protein expression on drug-drug interactions. *J Med Chem* **55**:4740-4763.

Khamdang S, Takeda M, Noshiro R, Narikawa S, Enomoto A, Anzai N, Piyachaturawat P and Endou H (2002) Interactions of human organic anion transporters and human organic cation transporters with nonsteroidal anti-inflammatory drugs. *J Pharmacol Exp Ther* **303**:534-539.

Klein DM and Cherrington NJ (2014) Organic and inorganic transporters of the testis: A review. *Spermatogenesis* **4**:e979653.

Kobayashi D, Nozawa T, Imai K, Nezu J, Tsuji A and Tamai I (2003) Involvement of human organic anion transporting polypeptide OATP-B (SLC21A9) in pH-dependent transport across intestinal apical membrane. *J Pharmacol Exp Ther* **306**:703-708.

Kouzuki H, Suzuki H and Sugiyama Y (2000) Pharmacokinetic study of the hepatobiliary transport of indomethacin. *Pharm Res* **17**:432-438.

Kullak-Ublick GA, Hagenbuch B, Stieger B, Schteingart CD, Hofmann AF, Wolkoff AW and Meier PJ (1995) Molecular and functional characterization of an organic anion transporting polypeptide cloned from human liver. *Gastroenterology* **109**:1274-1282.

Lee SY, Williamson B, Caballero OL, Chen YT, Scanlan MJ, Ritter G, Jongeneel CV, Simpson AJ and Old LJ (2004) Identification of the gonad-specific anion transporter SLCO6A1 as a cancer/testis (CT) antigen expressed in human lung cancer. *Cancer Immun* **4**:13.

Legendre A, Froment P, Desmots S, Lecomte A, Habert R and Lemazurier E (2010) An engineered 3D blood-testis barrier model for the assessment of reproductive toxicity potential. *Biomaterials* **31**:4492-4505.

Letschert K, Faulstich H, Keller D and Keppler D (2006) Molecular characterization and inhibition of amanitin uptake into human hepatocytes. *Toxicol Sci* **91**:140-149.

Leuthold S, Hagenbuch B, Mohebbi N, Wagner CA, Meier PJ and Stieger B (2009) Mechanisms of pH-gradient driven transport mediated by organic anion polypeptide transporters. *Am J Physiol Cell Physiol* **296**:C570-582.

Long JE, Lee MS and Blithe DL (2021) Update on novel hormonal and nonhormonal male contraceptive development. *J Clin Endocrinol Metab* **106**:e2381-e2392.

Matsson P, Pedersen JM, Norinder U, Bergstrom CA and Artursson P (2009) Identification of novel specific and general inhibitors of the three major human ATP-binding cassette transporters P-gp, BCRP and MRP2 among registered drugs. *Pharm Res* **26**:1816-1831.

Meier PJ, Eckhardt U, Schroeder A, Hagenbuch B and Stieger B (1997) Substrate specificity of sinusoidal bile acid and organic anion uptake systems in rat and human liver. *Hepatology* **26**:1667-1677.

Miller SR and Cherrington NJ (2018) Transepithelial transport across the blood-testis barrier. *Reproduction* **156**:R187-R194.

Miller SR, Hau RK, Jilek JL, Morales MN, Wright SH and Cherrington NJ (2020) Nucleoside Reverse Transcriptase Inhibitor Interaction with Human Equilibrative Nucleoside Transporters 1 and 2. *Drug Metab Dispos* **48**:603-612.

Miller SR, Zhang X, Hau RK, Jilek JL, Jennings EQ, Galligan JJ, Foil DH, Zorn KM, Ekins S, Wright SH and Cherrington NJ (2021) Predicting drug interactions with human Equilibrative Nucleoside Transporters 1 and 2 using functional knockout cell lines and Bayesian modeling. *Mol Pharmacol* **99**:147-162.

Mogilner JG, Lurie M, Coran AG, Nativ O, Shiloni E and Sukhotnik I (2006) Effect of diclofenac on germ cell apoptosis following testicular ischemia-reperfusion injury in a rat. *Pediatr Surg Int* **22**:99-105.

Mok KW, Mruk DD, Lie PP, Lui WY and Cheng CY (2011) Adjudin, a potential male contraceptive, exerts its effects locally in the seminiferous epithelium of mammalian testes. *Reproduction* **141**:571-580.

Moskovitz B, Munichor M and Levin DR (1987) Effect of diclofenac sodium (Voltaren) and prostaglandin E2 on spermatogenesis in mature dogs. *Eur Urol* **13**:393-396.

Mruk DD and Cheng CY (2015) The mammalian blood-testis barrier: its biology and regulation. *Endocr Rev* **36**:564-591.

Mruk DD, Su L and Cheng CY (2011) Emerging role for drug transporters at the blood-testis barrier. *Trends Pharmacol Sci* **32**:99-106.

Nozawa T, Imai K, Nezu J, Tsuji A and Tamai I (2004) Functional characterization of pH-sensitive organic anion transporting polypeptide OATP-B in human. *J Pharmacol Exp Ther* **308**:438-445.

Othman AI, El-Missiry MA and Amer MA (2001) The protective action of melatonin on indomethacin-induced gastric and testicular oxidative stress in rats. *Redox Rep* **6**:173-177.

Patik I, Kovacsics D, Nemet O, Gera M, Varady G, Stieger B, Hagenbuch B, Szakacs G and Ozvegy-Laczka C (2015) Functional expression of the 11 human Organic Anion Transporting Polypeptides in insect cells reveals that sodium fluorescein is a general OATP substrate. *Biochem Pharmacol* **98**:649-658.

Roth M, Obaidat A and Hagenbuch B (2012) OATPs, OATs and OCTs: the organic anion and cation transporters of the SLCO and SLC22A gene superfamilies. *Br J Pharmacol* **165**:1260-1287.

Sandoval PJ, Morales M, Secomb TW and Wright SH (2019) Kinetic basis of metformin-MPP interactions with organic cation transporter OCT2. *Am J Physiol Renal Physiol* **317**:F720-F734.

Sandoval PJ, Zorn KM, Clark AM, Ekins S and Wright SH (2018) Assessment of substrate-dependent ligand interactions at the organic cation transporter OCT2 using six model substrates. *Mol Pharmacol* **94**:1057-1068.

Satlin LM, Amin V and Wolkoff AW (1997) Organic anion transporting polypeptide mediates organic anion/HCO3- exchange. *J Biol Chem* **272**:26340-26345.

Sato R, Akiyoshi T, Morita T, Katayama K, Yajima K, Kataoka H, Imaoka A and Ohtani H (2021) Dual kinetics of OATP2B1: Inhibitory potency and pH-dependence of OATP2B1 inhibitors. *Drug Metab Pharmacokinet* **41**:100416.

Severance AC, Sandoval PJ and Wright SH (2017) Correlation between apparent substrate affinity and OCT2 transport turnover. *J Pharmacol Exp Ther* **362**:405-412.

Shitara Y, Sugiyama D, Kusuhara H, Kato Y, Abe T, Meier PJ, Itoh T and Sugiyama Y (2002) Comparative inhibitory effects of different compounds on rat oatpl (slc21a1)- and Oatp2 (Slc21a5)-mediated transport. *Pharm Res* **19**:147-153.

Shoop J, Holets L, Jakkaraj S, Georg G, Flynn C, Baltezor M, Tash J and Hagenbuch B (2014) The orally active male contraceptive agent H2-gamendazole interacts with organic anion transporting polypeptides expressed in human hepatocytes (1064.18). *The FASEB Journal* **28**:1064.1018.

Su L, Cheng CY and Mruk DD (2009) Drug transporter, P-glycoprotein (MDR1), is an integrated component of the mammalian blood-testis barrier. *Int J Biochem Cell Biol* **41**:2578-2587.

Su L, Mruk DD, Lee WM and Cheng CY (2011) Drug transporters and blood--testis barrier function. *J Endocrinol* **209**:337-351.

Sundar SV, Zhou X, Magenheimer BS, Reif GA, Wallace DP, Georg GI, Jakkaraj SR, Tash JS, Yu ASL, Li X and Calvet JP (2020) The Ionidamine derivative H2-gamendazole reduces cyst formation in polycystic kidney disease. *bioRxiv*:2020.2009.2009.258160.

Suzuki T, Onogawa T, Asano N, Mizutamari H, Mikkaichi T, Tanemoto M, Abe M, Satoh F, Unno M, Nunoki K, Suzuki M, Hishinuma T, Goto J, Shimosegawa T, Matsuno S, Ito S and Abe T (2003) Identification and characterization of novel rat and human gonad-specific organic anion transporters. *Mol Endocrinol* **17**:1203-1215.

Tash JS, Attardi B, Hild SA, Chakrasali R, Jakkaraj SR and Georg GI (2008a) A novel potent indazole carboxylic acid derivative blocks spermatogenesis and is contraceptive in rats after a single oral dose. *Biol Reprod* **78**:1127-1138.

Tash JS, Chakrasali R, Jakkaraj SR, Hughes J, Smith SK, Hornbaker K, Heckert LL, Ozturk SB, Hadden MK, Kinzy TG, Blagg BS and Georg GI (2008b) Gamendazole, an orally active indazole carboxylic acid male contraceptive agent, targets HSP90AB1 (HSP90BETA) and EEF1A1 (eEF1A), and stimulates Il1a transcription in rat Sertoli cells. *Biol Reprod* **78**:1139-1152.

Trussell J (2011) Contraceptive failure in the United States. *Contraception* **83**:397-404.

Vyas A, Purohit A and Ram H (2019) Assessment of dose-dependent reproductive toxicity of diclofenac sodium in male rats. *Drug Chem Toxicol* **42**:478-486.

Wang H, Chen XX, Wang LR, Mao YD, Zhou ZM and Sha JH (2010) AF-2364 is a prospective spermicide candidate. *Asian J Androl* **12**:322-335.

Westholm DE, Stenehjem DD, Rumbley JN, Drewes LR and Anderson GW (2009) Competitive inhibition of organic anion transporting polypeptide 1c1-mediated thyroxine transport by the fenamate class of nonsteroidal antiinflammatory drugs. *Endocrinology* **150**:1025-1032.

Zamek-Gliszczynski MJ, Sangha V, Shen H, Feng B, Wittwer MB, Varma MVS, Liang X, Sugiyama Y, Zhang L, Bendayan R and International Transporter C (2022) Transporters in drug development: International transporter consortium update on emerging transporters of clinical importance. *Clin Pharmacol Ther*. doi:10.1002/cpt.2644

Zhang X, Groves CE, Bahn A, Barendt WM, Prado MD, Rodiger M, Chatsudthipong V, Burckhardt G and Wright SH (2004) Relative contribution of OAT and OCT transporters to organic electrolyte transport in rabbit proximal tubule. *Am J Physiol Renal Physiol* **287**:F999-1010.

Zimmerli B, Valantinas J and Meier PJ (1989) Multispecificity of Na+-dependent taurocholate uptake in basolateral (sinusoidal) rat liver plasma membrane vesicles. *J Pharmacol Exp Ther* **250**:301-308.

Footnotes

This work was supported by funding from the National Institutes of General Medical Sciences [Grants R01GM123643 and R01GM129777], National Institute of Environmental Health Sciences [Grants R01ES028668 and T32ES007091], National Cancer Institute [Grant P30CA023074], and National Institute of Child Health and Human Development [Contract HHSN275201300017C]. The authors declare no conflicts of interest.

Citation of Meeting Abstracts

Hau, R., Georg, G., Wright, S., & Cherrington, N. (2022). Characterization of the Transporter-Mediated Uptake of the Experimental Male Contraceptive H2-Gamendazole. In: 2022 Annual Meeting Abstract Supplement, Society of Toxicology, 2022. Abstract no. #4345.

Hau, R., Miller, S., Yu, A., Georg, G., Wright, S., & Cherrington, N. (2021). Transporter-Mediated Uptake of the Reversible Male Contraceptive H2-Gamendazole Across the Human Blood-Testis Barrier. In: 2021 Annual Meeting Abstract Supplement, Society of Toxicology, 2021. Abstract no. 2729.

Reprint Requests

Nathan J. Cherrington, Department of Pharmacology & Toxicology, College of Pharmacy, University of Arizona, Tucson, AZ 85721. Email: cherring@pharmacy.arizona.edu

Figure Legends

Figure 1: Apparent kinetics of total transporter-mediated uptake of H2-GMZ in hT-SerCs and primary rat SCs. Michaelis-Menten kinetics of total transporter-mediated uptake of H2-GMZ in (A) hT-SerCs and (B) primary rat SCs. The solid line (uncorrected) was fitted to the raw data using equation 1 and reflects the combined effect of transporter-mediated uptake of H2-GMZ and a first-order component. The red dashed line (corrected) was fitted to the remaining data using equation 2. The chemical structure of H2-GMZ is shown in panel A. Data are represented as mean ± S.D.

Figure 2: Apparent kinetics of total transporter-mediated uptake of indazole carboxylic acid analogs in hT-SerCs. Michaelis-Menten kinetics of total transporter-mediated uptake of (A) GMZ, (B) JWS-2-112, (C) JWS-2-176, (D) RC-MC-100, and (E) RC-MC-241 in hT-SerCs. The solid line (uncorrected) was fitted to the raw data using equation 1 and reflects the combined effect of transporter-mediated uptake of each analog and a first-order component. The red dashed line (corrected) was fitted to the remaining data using equation 2. The chemical structures of each analog are shown in their respective panels. The maximum tested concentration of each analog was as follows: GMZ (1000 μM), JWS-2-176 (100 μM), and the remaining analogs (150 μM). Data are represented as mean ± S.D.

Figure 3: Inhibition of total transporter-mediated uptake of H2-GMZ by common transporter substrates and inhibitors in hT-SerCs. (A) Inhibitory effect of common transporter substrates or inhibitors co-incubated with 30 μM H2-GMZ on monolayers of

hT-SerCs. (B) Inhibitory effect of 1 mM indomethacin, diclofenac, and MK-571 co-incubated with 30 μM H2-GMZ. (C) Inhibitory effect of indazole carboxylic acid analogs co-incubated with 30 μM H2-GMZ. Intracellular accumulation of H2-GMZ was measured after 5 min in all experiments. Data are represented as mean ± S.D. An ordinary one-way ANOVA with Bonferroni's multiple comparison correction was used to determine statistical significance between the control and inhibitor groups. Significance is indicated as *: $p \leq 0.05$, **: $p \leq 0.01$, ***: $p \leq 0.001$, and ****: $p \leq 0.0001$.

Figure 4: pH-sensitivity and ion dependence of H2-GMZ transport into hT-SerCs. (A) Total intracellular accumulation of H2-GMZ in hT-SerCs using WB at pHs ranging from 6.5 to 8.0. (B) Total intracellular accumulation of H2-GMZ in hT-SerCs using four different transport buffers with WB acting as the control buffer. Potassium buffer inverted potassium and sodium concentrations to achieve high K^+ (135 mM) and low Na^+ (5 mM). Choline buffer completely replaced all sodium ions with choline ions. Sulfate buffer replaced all chloride ions with sulfate or hydroxide ions. Intracellular accumulation of H2-GMZ was measured after 5 min in all experiments. Data are represented as mean ± S.D. An ordinary one-way ANOVA with Bonferroni's multiple comparison correction was used to determine statistical significance between the control and test groups. Significance is indicated as *: $p \leq 0.05$, **: $p \leq 0.01$, ***: $p \leq 0.001$, and ****: $p \leq 0.0001$.

Figure 5: Apparent kinetics and inhibition of total transporter-mediated uptake of H2-GMZ in CHO, MDCK, and HEK-293 cells. Michaelis-Menten kinetics of total

transporter-mediated uptake of H2-GMZ in (A) CHO cells, (B) MDCK cells, and (C) HEK-293 cells. The solid line (uncorrected) was fitted to the raw data using equation 1 and reflects the combined effect of transporter-mediated uptake of each analog and a first-order component. The red dashed line (corrected) was fitted to the remaining data using equation 2. (D) Inhibitory effect of indomethacin, diclofenac, and MK-571 co-incubated with 30 μM H2-GMZ on monolayers of CHO, MDCK, or HEK-293 cells. Data are represented as mean ± S.D. An ordinary one-way ANOVA with Bonferroni's multiple comparison correction was used to determine statistical significance between the control and inhibitor groups. Significance is indicated as *: $p \leq 0.05$, **: $p \leq 0.01$, ***: $p \leq 0.001$, and ****: $p \leq 0.0001$.

Figure 6: IC_{50} analysis of H2-GMZ against human OATP1A2- and OATP2B1-mediated uptake of [^{3}H]E3S. Concentration-dependent inhibitory effect of H2-GMZ on human (A, C) OATP1A2- and (B, D) OATP2B1-mediated [^{3}H]E3S uptake (~15-20 nM) at (A, B) pH 7.4 or (C, D) pH 6.0. The solid line was fitted to the data using equation 3 and reflects the combined effect of transporter-mediated uptake of each analog and a first-order component. Total intracellular accumulation of H2-GMZ in (A) HEK-293-EV and HEK-293-OATP1A2 or (B) Flp-In CHO and CHO-OATP2B1 cells at pH 7.4 was measured by LC-MS/MS analysis. Intracellular accumulation of (A-D) [^{3}H]E3S or (E-F) H2-GMZ was measured after 5 min in all experiments. Data are represented as mean ± S.D and reported with 95% confidence intervals and with R^2 values for goodness of fit. An ordinary one-way ANOVA with Bonferroni's multiple comparison correction was used to determine statistical significance between the control cell line and overexpressing cell

line. Significance is indicated as *: $p \leq 0.05$, **: $p \leq 0.01$, ***: $p \leq 0.001$, and ****: $p \leq 0.0001$.

Tables

Table 1: List of MRM parameters for all compounds measured by LC-MS/MS.

Analyte	ESI	Q1 (m/z)	Q3 (m/z)	Declustering Potential (V)	Collision Energy (V)
H2-Gamendazole	Negative	415	225	-80	-26
			211	-80	-30
			159	-70	-29
JWS-2-112	Negative	429	85.1	-100	-53
JWS-2-176	Negative	346	302	-80	-25
			239	-85	-38
			177	-70	-30
RC-MC-100	Negative	387	343	-7	-15
			197	-7	-27
			170	-7	-29
RC-MC-241	Negative	413	333	-80	-25
			210	-80	-28
			182	-80	-42
Indomethacin	Positive	358	139	76	45
			111	71	71
Diclofenac	Positive	296	250	5	21
			215	5	27
Trofosfamide	Positive	323	154.1	35	37

JPET Fast Forward. Published on July 2, 2022 as DOI: 10.1124/jpet.122.001195
This article has not been copyedited and formatted. The final version may differ from this version.

Table 2: Summary of kinetic parameters including standard deviations for H2-GMZ and other indazole carboxylic acid analogs in tested cells.

Compound	Cell	$J_{max\text{-}app}$ (pmol/cm^2•min)	$K_{t\text{-}app}$ (μM)
H2-GMZ	hT-SerC	266 ± 112	138 ± 39.3
	Primary rat SC	259 ± 62.9	151 ± 43.2
	CHO	804 ± 108	160 ± 28.1
	MDCK	1040 ± 384	121 ± 57.6
	HEK-293	2810 ± 613	472 ± 153
GMZ	hT-SerC	232 ± 56.5	38.3 ± 1.28
JWS-2-112		283 ± 80.2	48.0 ± 1.32
JWS-2-176		N/A	N/A
RC-MC-100		197 ± 15.1	83.0 ± 30.6
RC-MC-241		179 ± 39.5	25.5 ± 6.03

JPET Fast Forward. Published on July 2, 2022 as DOI: 10.1124/jpet.122.001195
This article has not been copyedited and formatted. The final version may differ from this version.

Figure 1

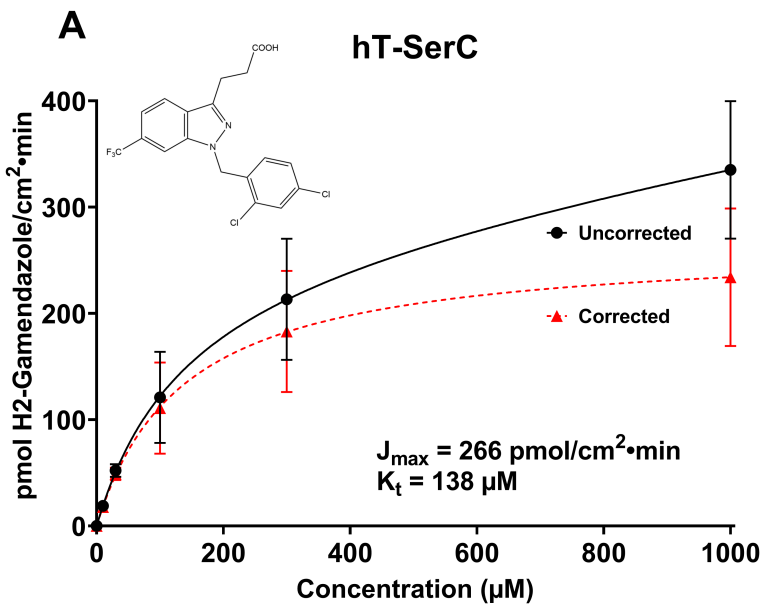

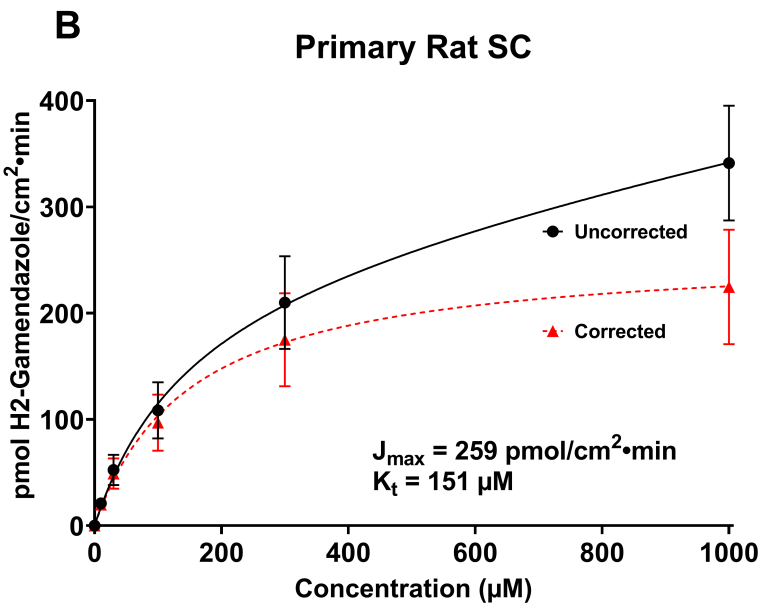

JPET Fast Forward. Published on July 2, 2022 as DOI: 10.1124/jpet.122.001195
This article has not been copyedited and formatted. The final version may differ from this version.

Figure 2

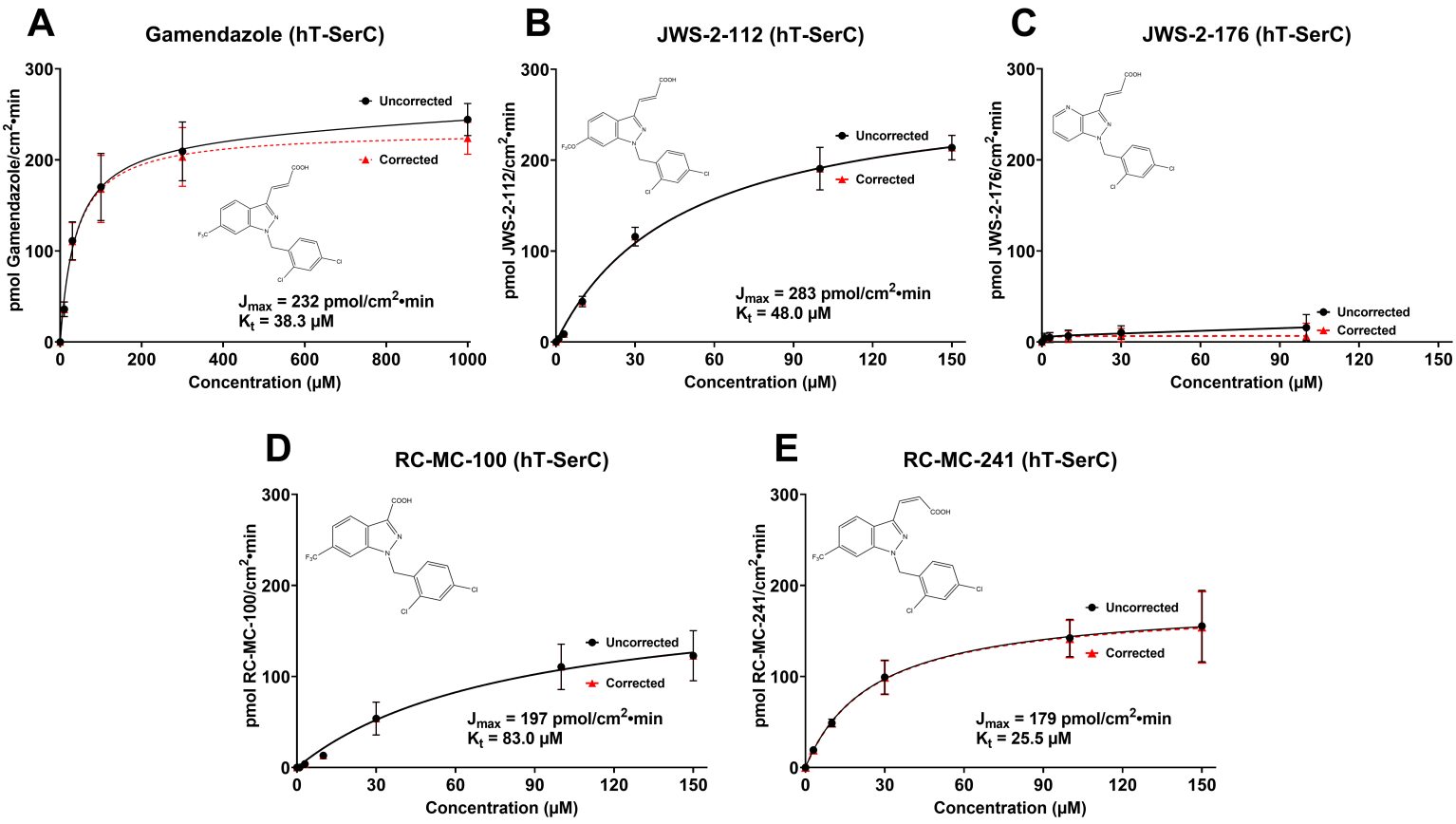

JPET Fast Forward. Published on July 2, 2022 as DOI: 10.1124/jpet.122.001195
This article has not been copyedited and formatted. The final version may differ from this version.

Figure 3

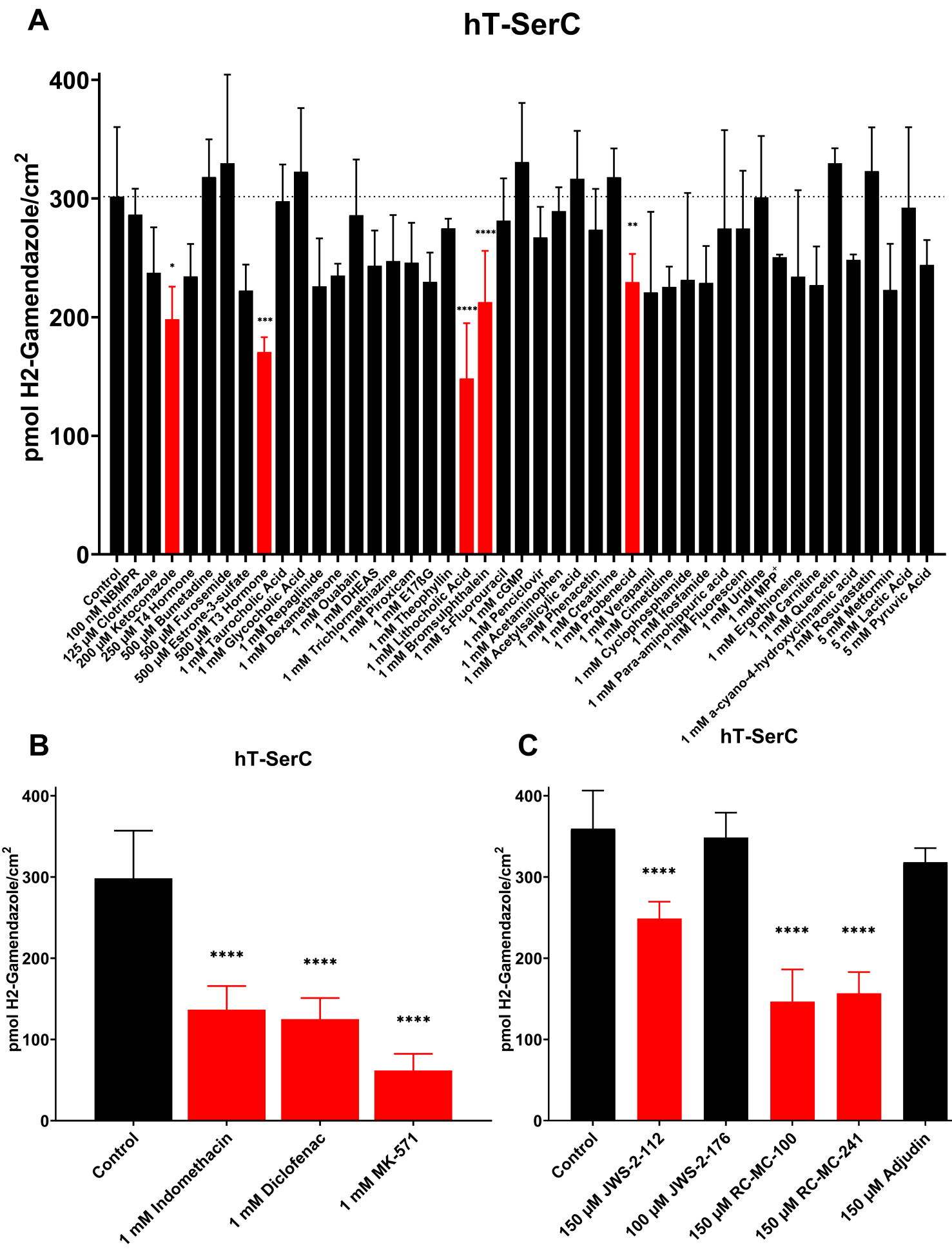

JPET Fast Forward. Published on July 2, 2022 as DOI: 10.1124/jpet.122.001195
This article has not been copyedited and formatted. The final version may differ from this version.

Figure 4

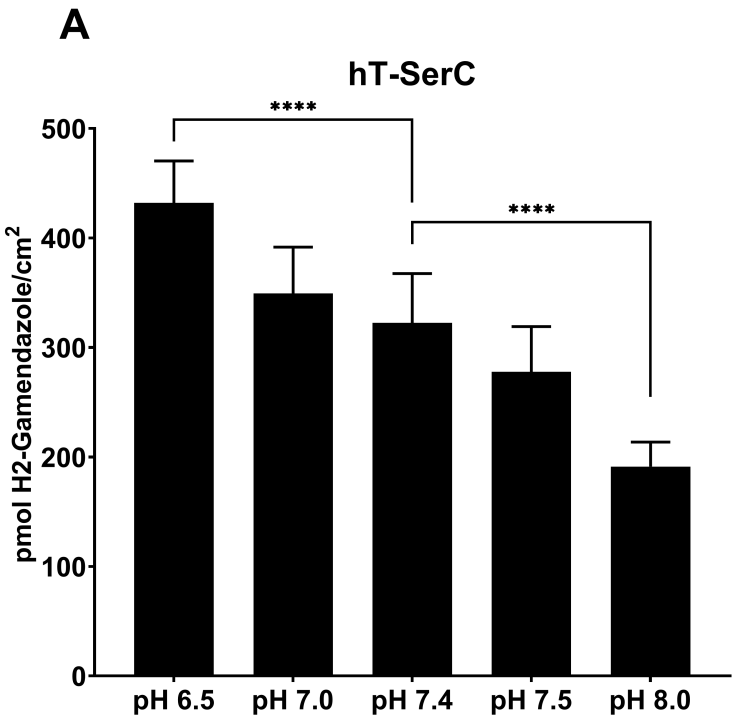

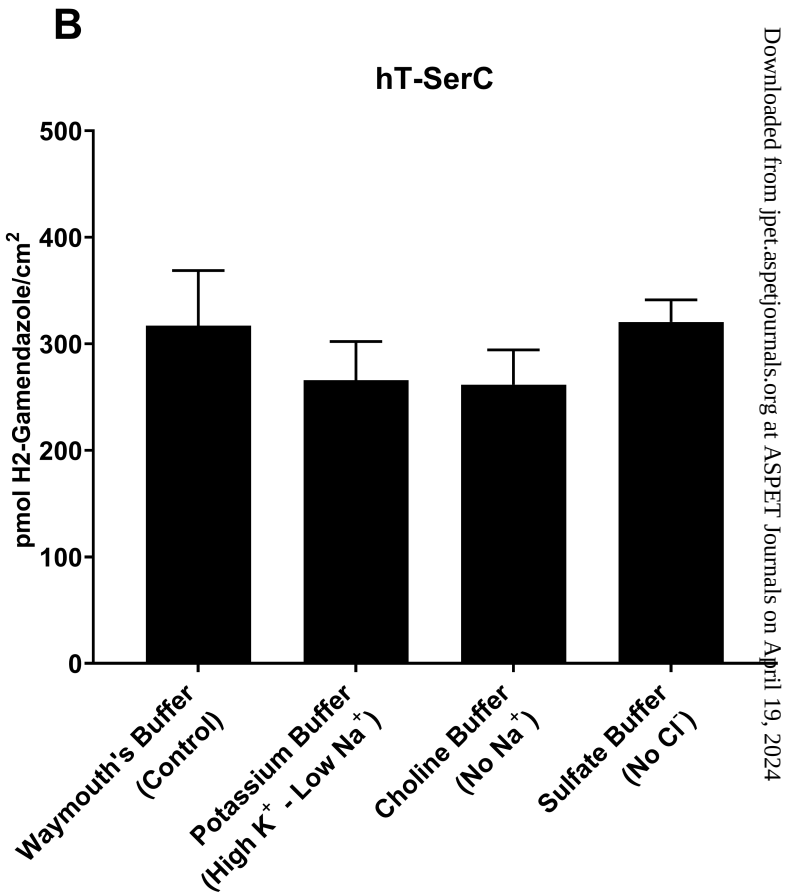

JPET Fast Forward. Published on July 2, 2022 as DOI: 10.1124/jpet.122.001195
This article has not been copyedited and formatted. The final version may differ from this version.

Figure 5

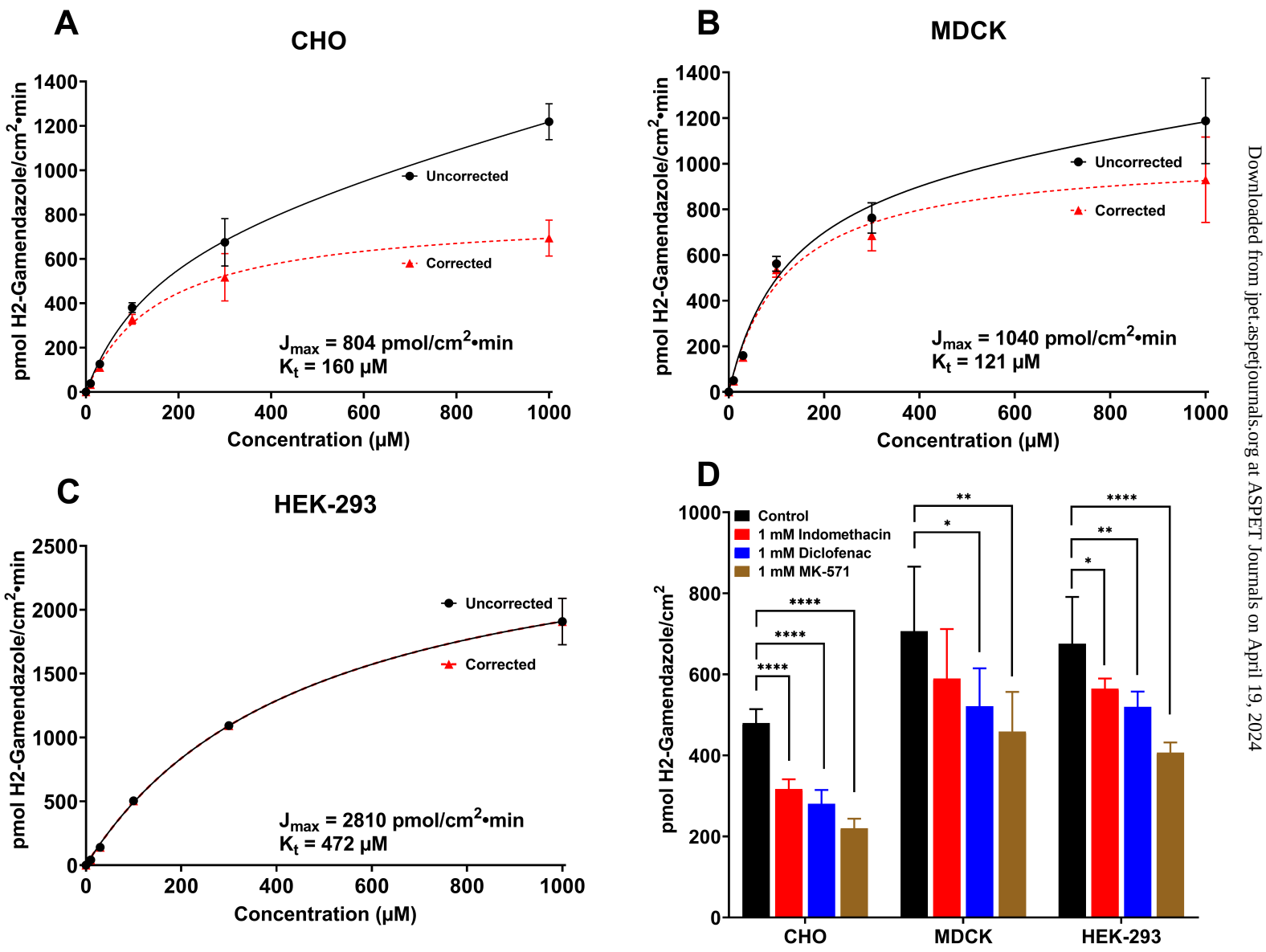

JPET Fast Forward. Published on July 2, 2022 as DOI: 10.1124/jpet.122.001195
This article has not been copyedited and formatted. The final version may differ from this version.

Figure 6